Approaching Monocoordination at a Silver(I) Cation

Matthew M. D. Roy, Michael J. Ferguson, Robert McDonald, Eric Rivard*

Contents:

Complete Experimental Procedures

X-Ray Crystallographic Data

Computational Data

General

All reactions were performed in an inert atmosphere glovebox (Innovative Technology, Inc.). Solvents were dried using a Grubbs-type solvent purification system[1] manufactured by Innovative Technologies, Inc., degassed (freeze-pump-thaw method), and stored under an atmosphere of nitrogen prior to use. All reactions were conducted in the absence of light until the products were isolated as solids. Na[BAr$^F_4$] was purchased from Ark Pharmaceuticals and dried by heating to 110 °C under vacuum for two days prior to use. Crotonaldehyde was purchased from Sigma Aldrich, degassed and dried over molecular sieves for 2 days (to remove H_2O stabilizer) prior to use. AgOTf was purchased from Matrix Scientific and used as received. ITr [$(HCNCPh_3)_2C$:] was prepared according a modified literature procedure[2] where the workup of the [ITrH]OTf precursor was conducted under inert atmosphere. Na[PCO](dioxane)$_{2.5}$ was synthesized according to the literature procedure and its dioxane content was determined as described.[3] ^{1}H, ^{11}B{^{1}H}, ^{13}C{^{1}H}, ^{19}F and ^{31}P{^{1}H} NMR spectra were recorded on 400, 500, 600 or 700 MHz Varian Inova instruments and were referenced externally to $SiMe_4$ (^{1}H, ^{13}C{^{1}H}), $CFCl_3$ (^{19}F), $F_3B{\cdot}OEt_2$ (^{11}B{^{1}H}), or 85 % H_3PO_4 (^{31}P{^{1}H}). Elemental analyses were performed by the Analytical and Instrumentation Laboratory at the University of Alberta. Melting points were measured in sealed glass capillaries under nitrogen using a MelTemp apparatus.

X-ray Crystallography

Crystals for X-ray diffraction studies were removed from a vial (in a glovebox) and immediately coated with a thin layer of hydrocarbon oil (Paratone-N). A suitable crystal was then mounted on a glass fiber and quickly placed in a low temperature stream of nitrogen on the X-ray diffractometer.[4] All data were collected using a Bruker APEX II CCD detector/D8 or PLATFORM diffractometer using Mo Kα or Cu Kα radiation, with the crystals cooled to – 80 °C or – 100 °C. The data were corrected for absorption through Gaussian integration from the indexing of the crystal faces. Crystal structures were solved using intrinsic phasing (*SHELXT*)[5] and refined using *SHELXL-2014*.[6] The assignment of hydrogen atom positions were based on the sp^2 or sp^3 hybridization geometries of their attached carbon atoms and were given thermal parameters 20% greater than those of their parent atoms.

Synthesis of [(ITr)Ag(OTf)] (1):

A *ca.* 10 mL solution of ITr (0.197 g, 0.356 mmol) in toluene was added to a vial containing AgOTf (0.090 g, 0.35 mmol). The resulting white slurry was stirred for 2 hours and the volatiles removed *in vacuo* affording [(ITr)Ag(OTf)] as an off-white solid (0.263 g, 93 %). Crystals suitable for X-ray crystallographic analysis were obtained by layering a fluorobenzene solution of **1** with hexanes and storing the mixture at-30 °C in a freezer overnight. ^{1}H NMR (C_6D_6, 499.8 MHz): δ 7.11-7.03 (m, 30H, Ar*H*), 6.52 (s, 2H, NC*H*). $^{13}C\{^1H\}$ NMR (C_6D_6, 128.0 MHz): δ 142.3 (Ar*C*), 130.0 (Ar*C*), 128.6 (Ar*C*), 128.5 (Ar*C*), 120.3 (N*C*H), 78.6 (*C*Ph$_3$). ^{19}F NMR (C_6D_6, 376.7 MHz): δ -77.1 (s). M.p. 187 °C (decomp.). Anal. Calcd. for $C_{42}H_{32}AgF_3N_2O_3S$: C 62.31, H 3.98, N 3.46, S 3.96. Found: C 62.32, H 4.04, N 3.47, S 3.74.

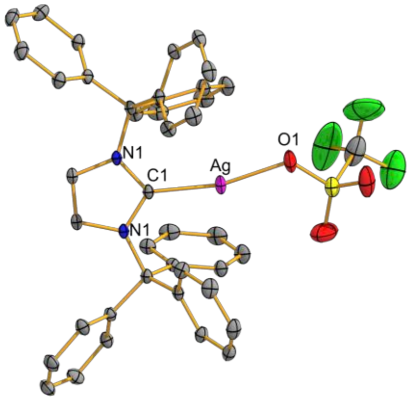

Figure S1. Molecular structure of [(ITr)Ag(OTf)] (**1**) with thermal ellipsoids plotted at the 30 % probability level. All hydrogen atoms have been omitted for clarity. Selected bond lengths [Å] and angles [°]: C1-Ag 2.097(3), Ag-O1 2.172(4); C1-Ag-O1 162.31(13).

Synthesis of [(ITr)Ag(PhF)][BAr^F$_4$] (3):

A *ca.* 12 mL fluorobenzene slurry of ITr (0.264 g, 0.478 mmol) was added to a vial containing AgOTf (0.119 g, 0.463 mmol). The resulting slurry was stirred for 1 hour and subsequently added to a vial containing Na[BAr^F$_4$] (0.410 g, 0.463 mmol). The reaction mixture was stirred for 1 hour and filtered. The filtrate was layered with an equal volume of hexanes and placed in a -30

°C freezer overnight, yielding pale yellow crystals of **3**, which were isolated and dried (0.519 g, 69 %). Crystals suitable for X-ray crystallographic analysis were obtained by layering a fluorobenzene solution of **3** with hexanes and storing the mixture at -30 °C in a freezer overnight.

Synthesis of [(ITr)Ag(MesH)][BAr^F$_4$] (4):

3 mL of mesitylene (MesH) was added to a vial containing [(ITr)Ag(OTf)] (0.065 g, 0.080 mmol) and Na[BAr^F$_4$] (0.072 g, 0.081 mmol). The resulting white slurry was stirred overnight and filtered. The filtrate was then layered with an equal volume of hexanes and placed in a -30 °C freezer overnight to give a few colorless crystals of **4** (0.007 g, <1% yield).

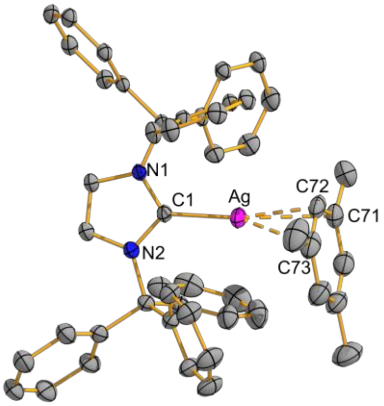

Figure S2. Molecular structure of [(ITr)Ag(MesH)][BAr^F$_4$] (**4**) with thermal ellipsoids plotted at the 30 % probability level. All hydrogen atoms and the [BAr^F$_4$]$^-$ counterion and free MesH solvate have been omitted for clarity. Selected bond lengths [Å] and angles [°]: C1-Ag 2.112(3), Ag-C71 2.682(4), Ag-C72 2.323(4), Ag-C73 2.719(5); C1-Ag-C71 152.65(14), C1-Ag-C72 168.86(13), C1-Ag-C73 152.47(15).

Synthesis of [(ITr)Ag(CH_2Cl_2)][$BAr^F{}_4$] (5) and [(ITr)Ag]$_2$[$BAr^F{}_4$]$_2$ (6):

A *ca.* 5 mL solution of [(ITr)Ag(OTf)] (0.127 g, 0.157 mmol) in CH_2Cl_2 was added to a vial containing Na[$BAr^F{}_4$] (0.139 g, 0.157 mmol). After 3 minutes, the resulting slurry began to take on a bright yellow color. The slurry was stirred for 1 hour and filtered. The filtrate was a bright yellow solution and the white precipitate was discarded. The filtrate was layered with an equal volume of hexanes and placed in a -30 °C freezer overnight, yielding yellow rod-shaped crystals and yellow block-like crystals. A few crystals were removed for X-ray crystallographic analysis and the rod-like crystals were determined to be **6** and the blocks were found to be **5**. The mother liquor was decanted, the crystals washed with 2 x 2 mL hexanes and the volatiles were removed *in vacuo* yielding a yellow crystalline solid (0.012 g, crop 1). The mother liquor was subsequently concentrated to half its original volume, layered with an equal volume of hexanes and placed in a -30 °C freezer for 1 week affording more yellow crystals. The mother liquor was decanted again, the crystals washed with 2 x 2 mL hexanes yielding a mixture of **5** and **6** as a yellow crystalline solid (0.145 g, crop 2). The two crops of crystals were then combined (0.157 g). Based on the crystal morphologies, the final product contains a mixture of **5** and **6**, and thus a fine yield is not listed. NMR analysis of the mixture in C_6D_6 gave data that was consistent with the formation of [(ITr)Ag(C_6D_6)][$BAr^F{}_4$].

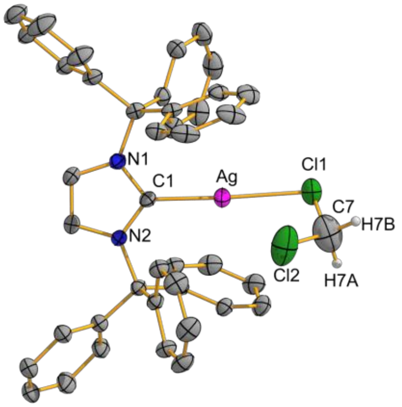

Figure S3. Molecular structure of [(ITr)Ag(CH_2Cl_2)$_{0.7}$(η^3-toluene)$_{0.3}$][BAr$^F_4$] with thermal ellipsoids plotted at the 30 % probability level. All hydrogen atoms (except for CH_2Cl_2), the [BAr$^F_4$]$^-$ counterion and the 30 % η^3-coordinated toluene molecule (in the form of [(ITr)Ag((η^3-toluene)][BAr$^F_4$]) have been omitted for clarity. Selected bond lengths [Å] and angles [°]: C1-Ag 2.098(4), Ag-Cl1 2.524(2); Cl-Ag-Cl1 170.64(12).

NMR data for [(ITr)Ag(C_6D_6)][BAr$^F_4$] and analytical data for "[(ITr)Ag][BAr$^F_4$]":

^{1}H, ^{13}C{^{1}H}, ^{11}B{^{1}H} and ^{19}F NMR spectroscopy for compounds **3**-**6** in C_6D_6 revealed identical NMR spectra, along with the corresponding free fluorobenzene (**3**), mesitylene (**4**) or dichloromethane (**5**) in the ^{1}H and ^{13}C{^{1}H} spectra indicating that compounds **3**-**6** are the same in C_6D_6 solution. To confirm the formation of [(ITr)Ag(C_6D_6)][BAr$^F_4$] the reaction of [(ITr)Ag(OTf)] and Na[BAr$^F_4$] was conducted in C_6D_6 solvent and an aliquot was filtered revealing the same traces in the NMR spectra as for when compounds **3**-**6** are dissolved in C_6D_6.

Data for [(ITr)Ag(C_6D_6)][BAr$^F_4$]: ^{1}H NMR (C_6D_6, 499.8 MHz): δ 8.40 (broad s, 8H, *o*-$C_6H_3(CF_3)_2$), 7.65 (broad s, 4H, *p*-$C_6H_3(CF_3)_2$), 7.00-6.95 (m, 6H, Ar*H*), 6.94-6.89 (m, 12H, Ar*H*), 6.70-6.64 (m, 12H, Ar*H*), 6.25 (broad d, 2H, $^4J_{\text{H-Ag}}$ = 1.9 Hz, NC*H*). ^{13}C{^{1}H} NMR (C_6D_6, 125.7 MHz): δ 163.0 (q, $^1J_{\text{CB}}$ = 47.8 Hz, *ipso*-$C_6H_3(CF_3)_2$), 141.9 (Ar*C*), 135.4 (Ar*C*), 129.6 (Ar*C*), 128.7 (Ar*C*), 128.4 (Ar*C*), 125.2 (q, $^1J_{\text{CF}}$ = 272.7 Hz, *C*F_3), 118.0 (broad, N*C*H), 78.1

(CPh$_3$). An NCN resonance was not observed. ^{19}F NMR (C$_6$D$_6$, 468.7 MHz): δ -62.1 (s, BAr$^F_4$). ^{11}B{^{1}H} (C$_6$D$_6$, 159.8 MHz): δ -5.9 (s, BAr$^F_4$).

Crystals of **5** and **6** were re-dissolved in CH$_2$Cl$_2$ and dried *in vacuo* for several hours yielding a yellow powder. NMR spectroscopy (in C$_6$D$_6$) revealed that all CH$_2$Cl$_2$ had been removed from the solid, and elemental analysis was found to be consistent with a product of the general formula [(ITr)Ag][BAr$^F_4$] (most likely the solvent-free dimer **6**).

M.p. 154 °C (decomp.). Anal. Calcd. for $C_{73}H_{44}AgBF_{24}N_2$: C 57.53, H 2.91, N 1.84. Found C 57.14, H 3.21, N 1.78.

Synthesis of [(ITr)Ag(PCO)] (7):

A *ca.* 2 mL solution of Na[PCO](diox)$_{2.5}$ (0.143 g, 0.177 mmol) in THF was added to a vial containing a *ca.* 2 mL THF solution of [(ITr)Ag(OTf)] (0.055 g, 0.182 mmol). The resulting slurry was stirred for 20 minutes and had turned a dark brown (originally white colored). The slurry was filtered yielding a dark brown solution. The filtrate was layered with an equal volume of hexanes and placed in a - 30 °C freezer overnight. The supernatant was decanted from the resulting brown precipitate and the precipitate washed 2 x 2 mL hexanes. The volatiles were removed *in vacuo* affording [(ITr)Ag(PCO)] as a brown powder (0.053 g, 42 %). Crystals suitable for X-ray crystallographic analysis were obtained by layering a THF solution of **7** with hexanes and storing in a -30 °C freezer overnight. ^{1}H NMR (C$_6$D$_6$, 400.0 MHz): δ 7.22-7.17 (m, ArH, 12H), 7.13-7.02 (m, ArH, 18H), 6.55 (broad s, 2H, NCH). ^{13}C{^{1}H} NMR (C$_6$D$_6$, 125.7 MHz): δ 172.8 (d, $^1J_{C\text{-}P}$ = 91.8 Hz, -PCO), 142.7 (ArC), 130.3 (ArC), 128.5 (ArC), 128.3 (ArC), 120.0 (broad s, NCH), 78.4 (CPh$_3$). An NCN resonance was not observed. ^{31}P{^{1}H} NMR (C$_6$D$_6$, 161.9 MHz): δ -406.0 (broad s). ^{31}P{^{1}H} NMR (toluene-d$_8$, 161.8 MHz, - 80°C): δ -304.8 (d, $^1J_{P\text{-}Ag}$ = 152.5 Hz). M.p. 135 °C (decomp.). Anal. Calcd. for $C_{42}H_{32}AgN_2OP$: C 70.11, H 4.48, N 3.89. Found: C 69.49, H 4.51, N 3.82.

Addition of Crotonaldehyde to “[(ITr)Ag][BAr^F]” (Childs Method for determining Lewis acidity):

To a vial containing a 1.5 mL CD_2Cl_2 solution of “[(ITr)Ag][BAr$^F{}_4$]” (likely containing a mixture of **5** and **6**, synthesized from **1** and Na[BAr$^F{}_4$] in CH_2Cl_2; 0.049 g, 0.032 mmol) was added *trans*-crotonaldehyde (2.7 µL, 0.033 mmol) in CD_2Cl_2. After stirring for 70 minutes an aliquot was removed for NMR analysis. ^{1}H NMR spectroscopy revealed a set of crotonaldehyde peaks shifted from free crotonaldehyde. ^{1}H NMR (CD_2Cl_2, 399.8 MHz): δ 9.12 (d, 1H, H1), 6.95 (m, 1H, H3), 5.78 (ddq, 1H, H2), 2.00 (dd, 3H, H4). Free cotonaldehyde: ^{1}H NMR (CD_2Cl_2, 399.8 MHz): δ 9.47 (d, 1H, H1), 6.87 (m, 1H, H3), 6.10 (ddq, 1H, H2), 2.10 (dd, 3H, H4). The chemical shift difference of the H3 proton between free and coordinated crotonaldehyde was found to be: Δδ H3 = 0.08 ppm.

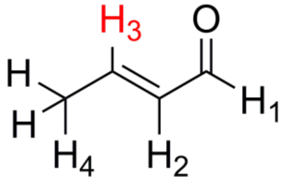

NMR Spectra

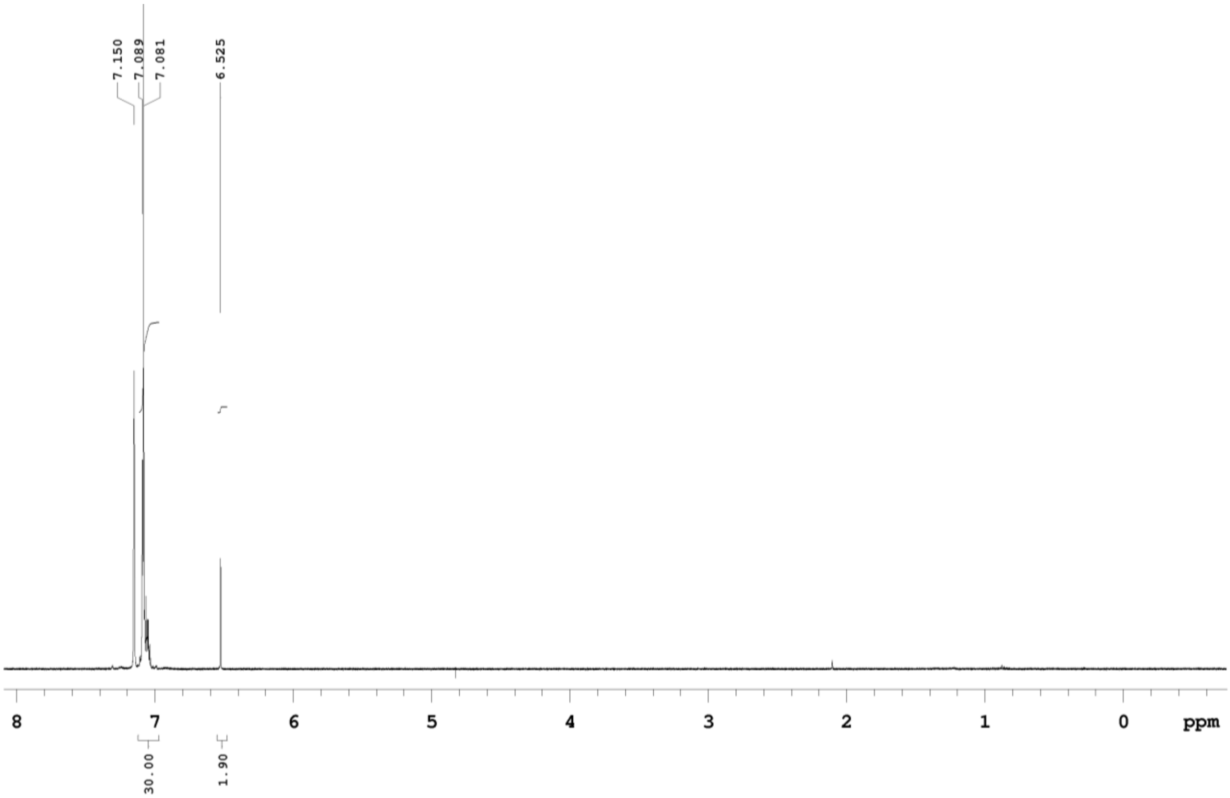

Figure S4. ^{1}H NMR spectrum of [(ITr)Ag(OTf)] (**1**) in C_6D_6.

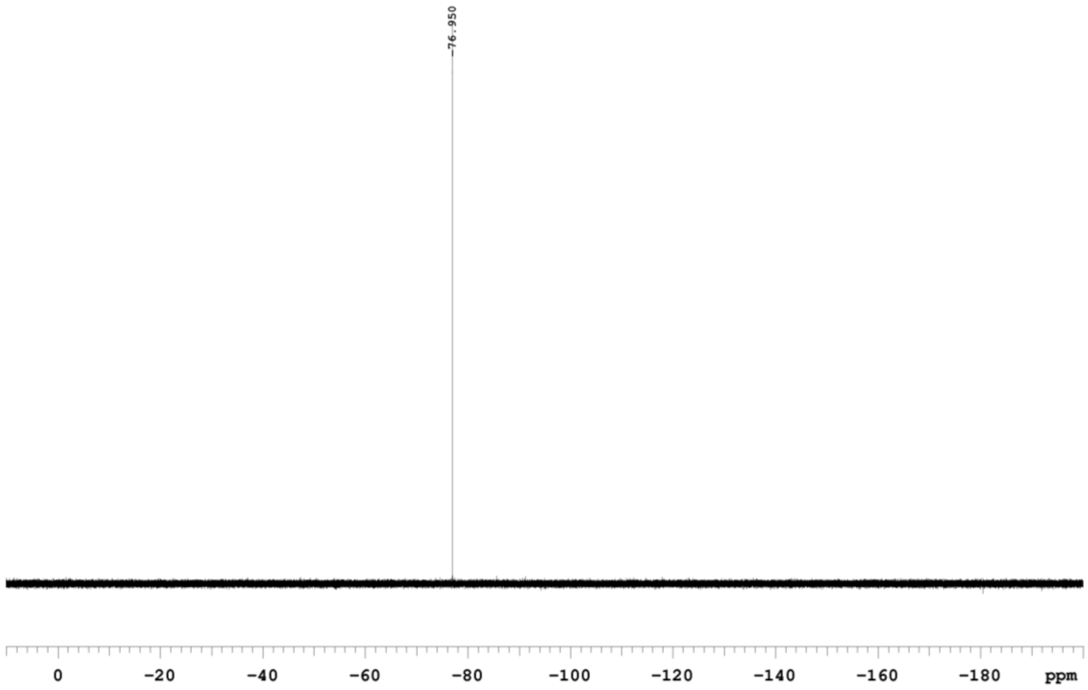

Figure S5. ^{19}F NMR spectrum of [(ITr)Ag(OTf)] (**1**) in C_6D_6.

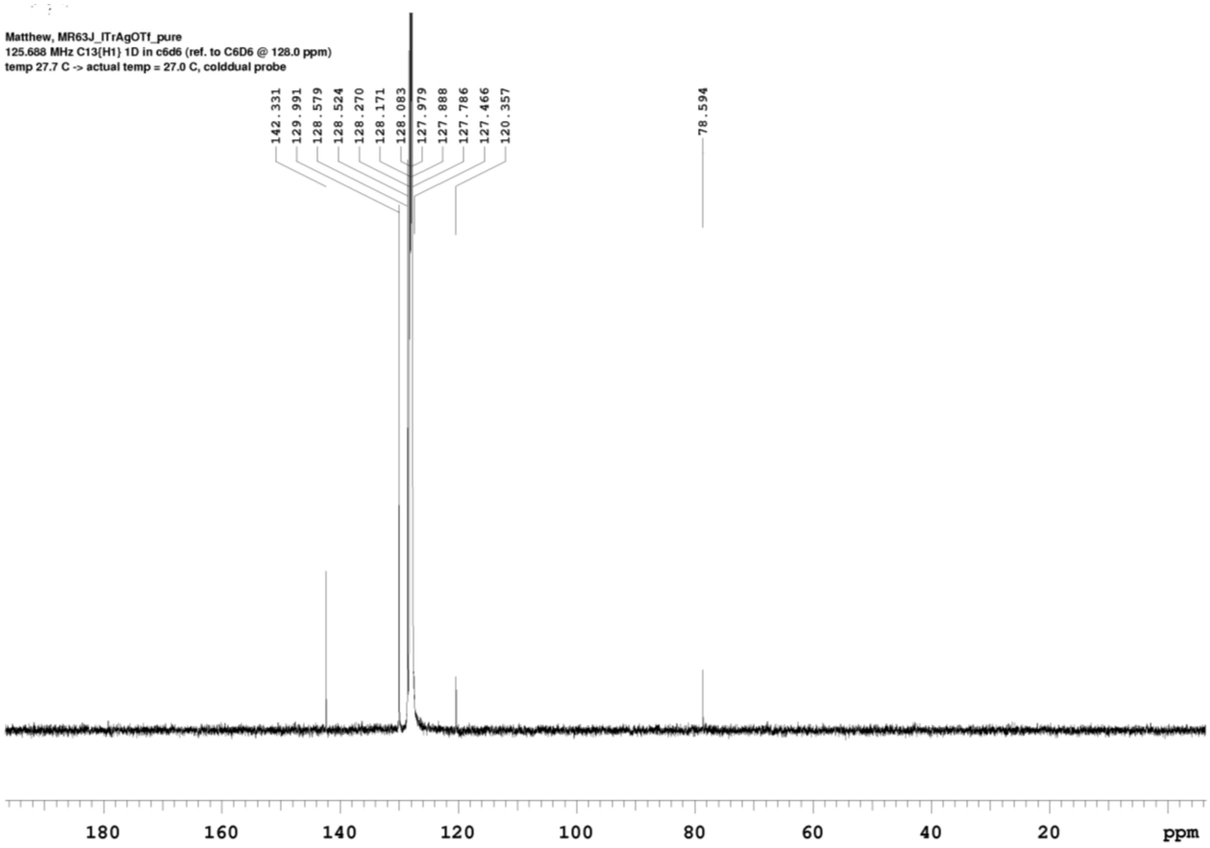

Figure S6. $^{13}C\{^1H\}$ NMR spectrum of [(ITr)Ag(OTf)] (**1**) in C_6D_6.

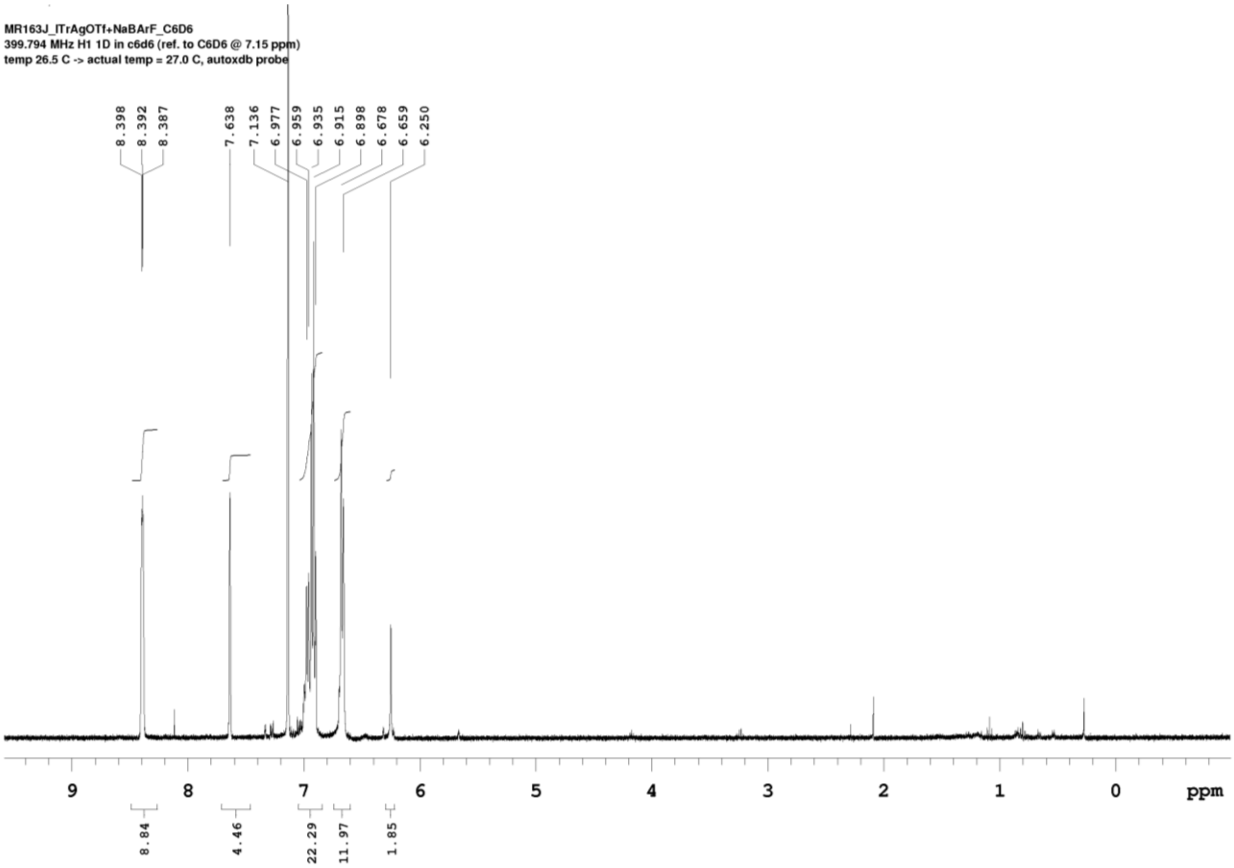

Figure S7. ^{1}H NMR spectrum of [(ITr)Ag(C_6D_6)][BAr$^F{}_4$] in C_6D_6.

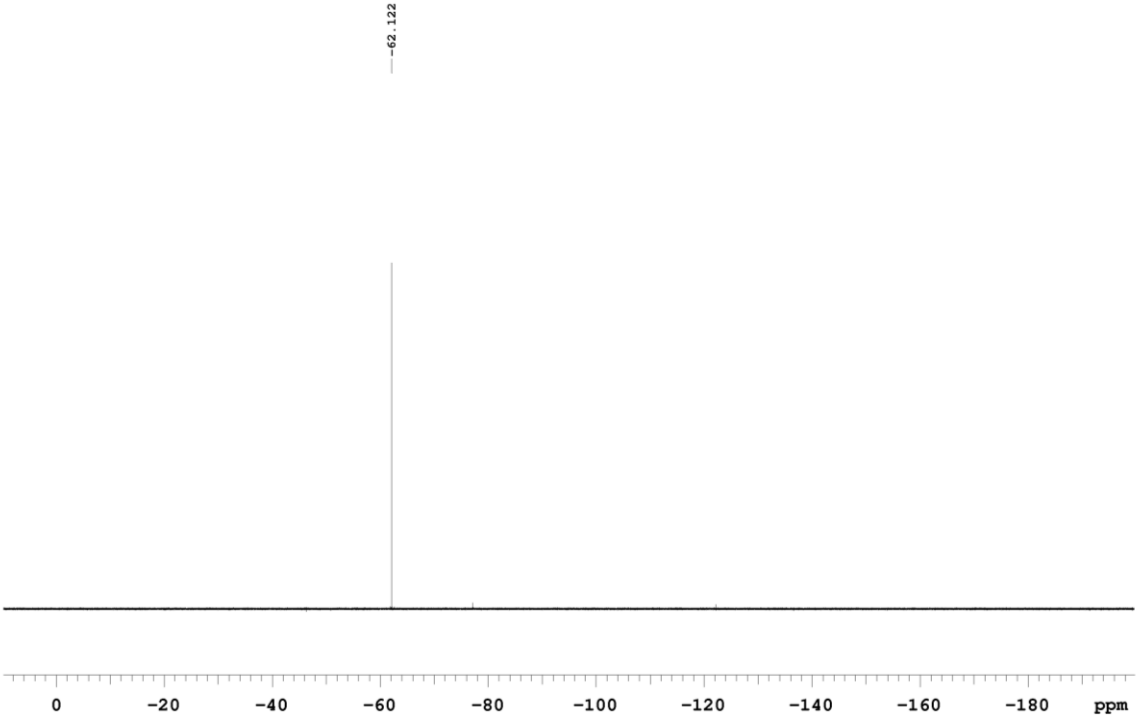

Figure S8. ^{19}F NMR spectrum of $[(\mathrm{ITr})\mathrm{Ag}(C_6D_6)][\mathrm{BAr^F}_4]$ in C_6D_6.

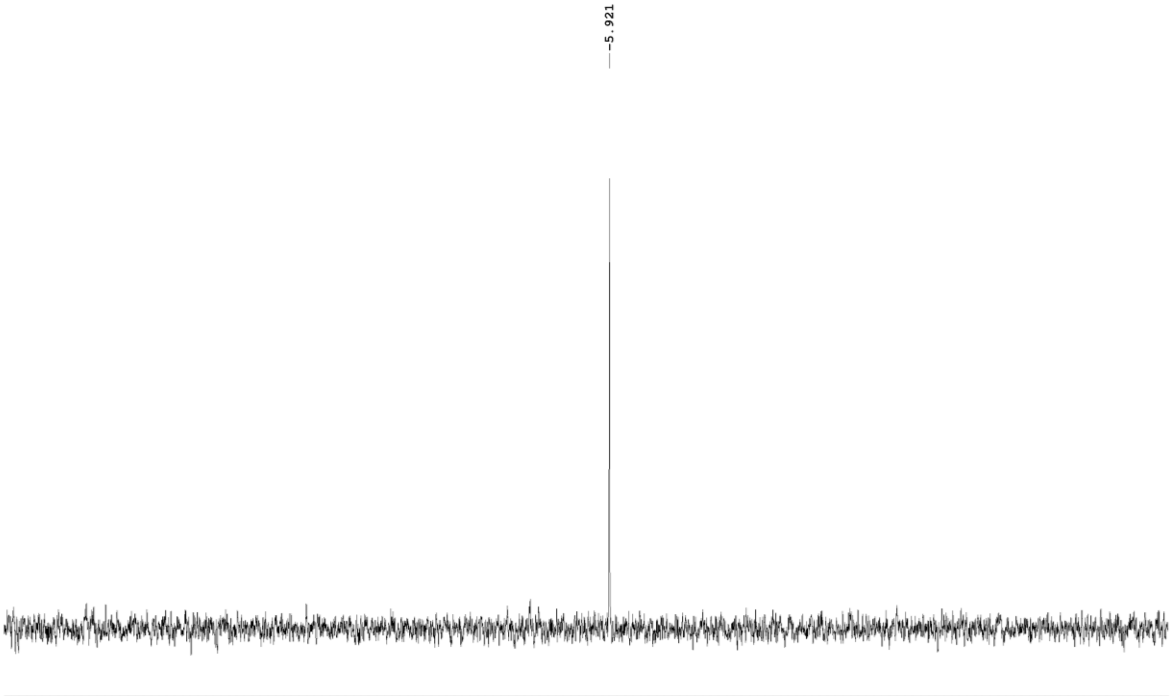

Figure S9. ^{11}B{^{1}H} NMR spectrum of $[(\mathrm{ITr})\mathrm{Ag}(C_6D_6)][\mathrm{BAr^F}_4]$ in C_6D_6.

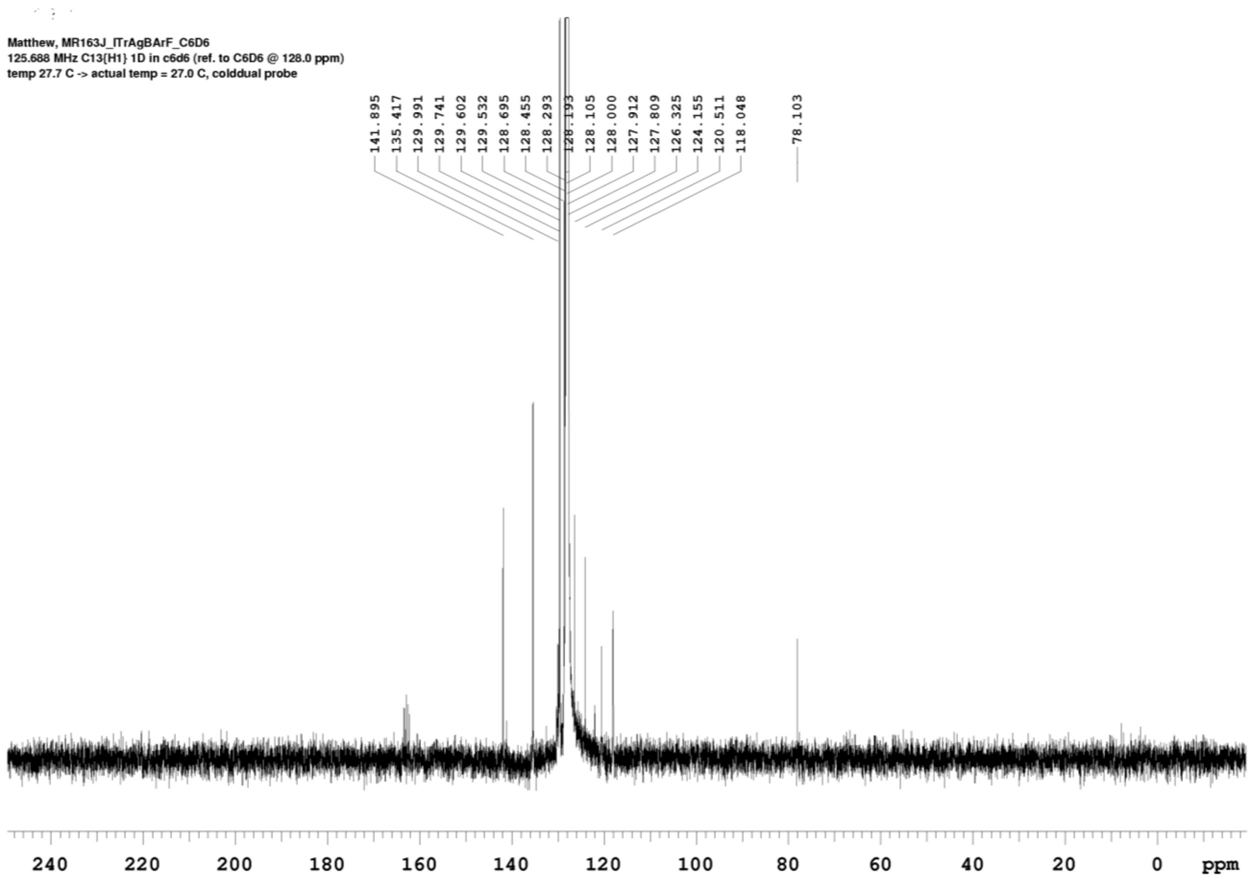

Figure S10. $^{13}C\{^1H\}$ NMR spectrum of $[(ITr)Ag(C_6D_6)][BAr^F{}_4]$ in C_6D_6.

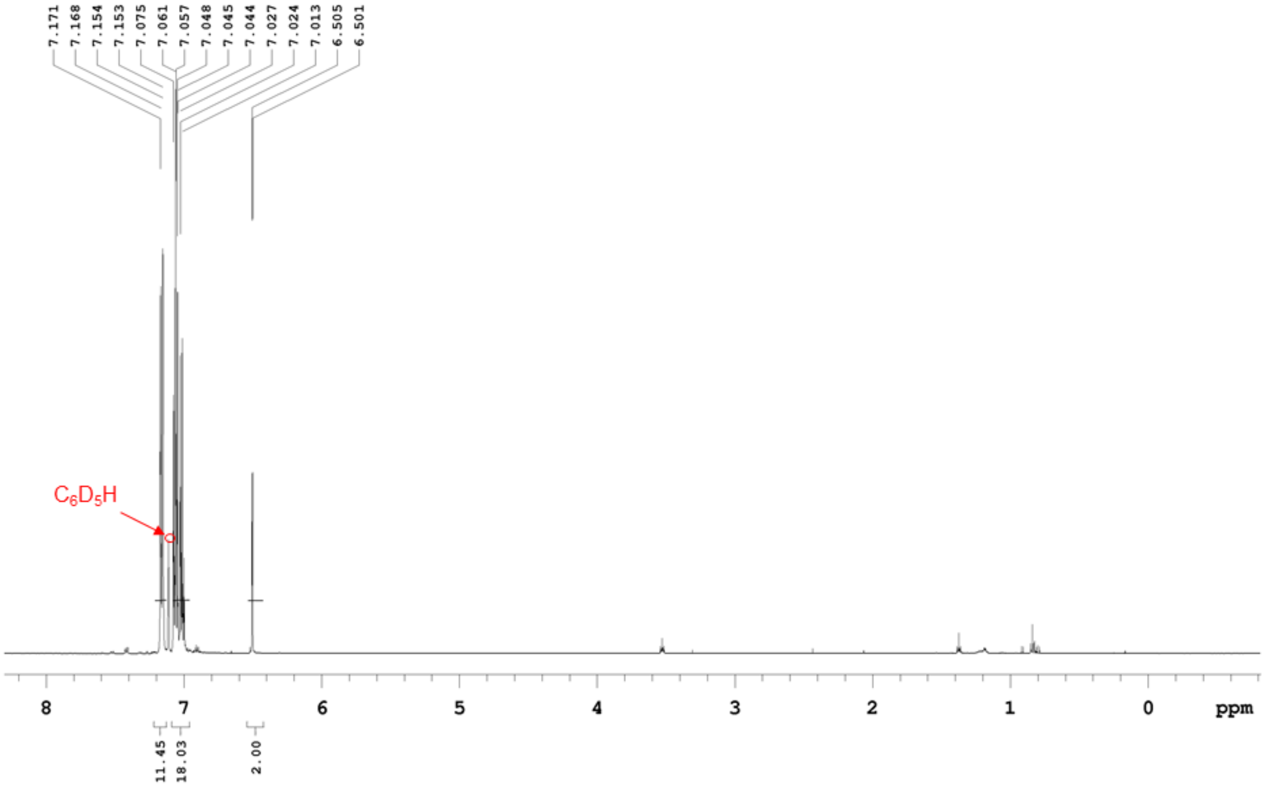

Figure S11. ^{1}H NMR spectrum of [(ITr)Ag(η^2-PCO)] (**7**) in C_6D_6.

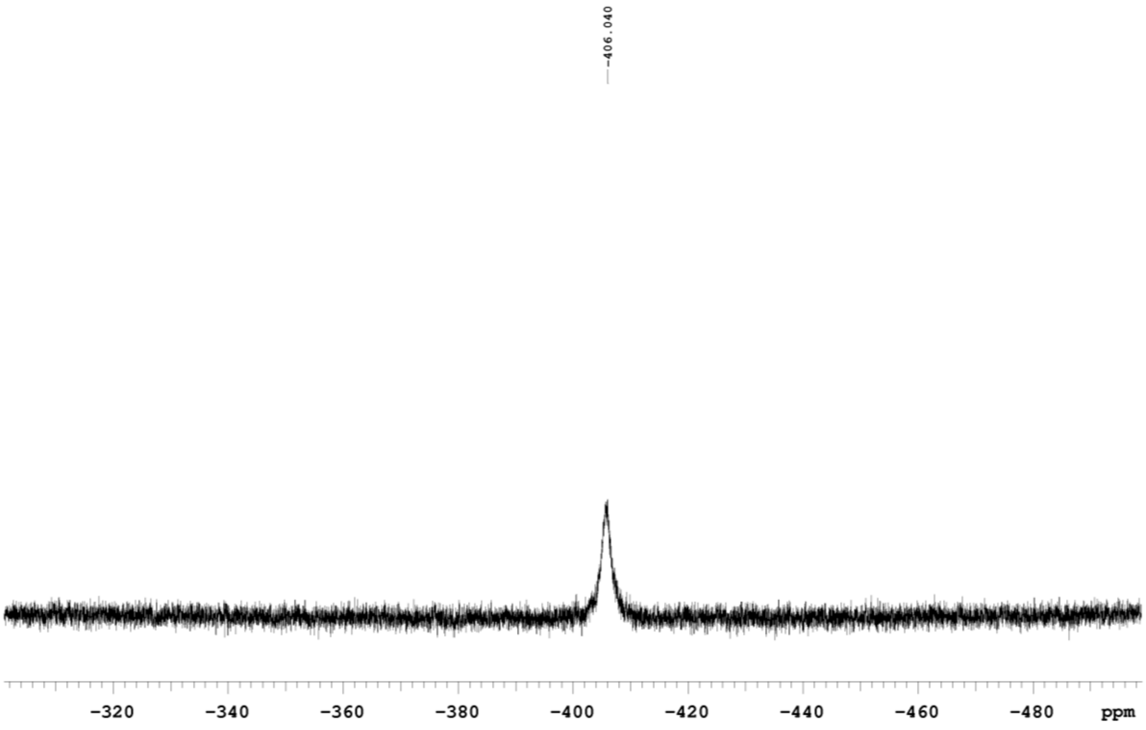

Figure S12. ^{31}P{^{1}H} NMR spectrum of [(ITr)Ag(η^2-PCO)] (**7**) in C_6D_6.

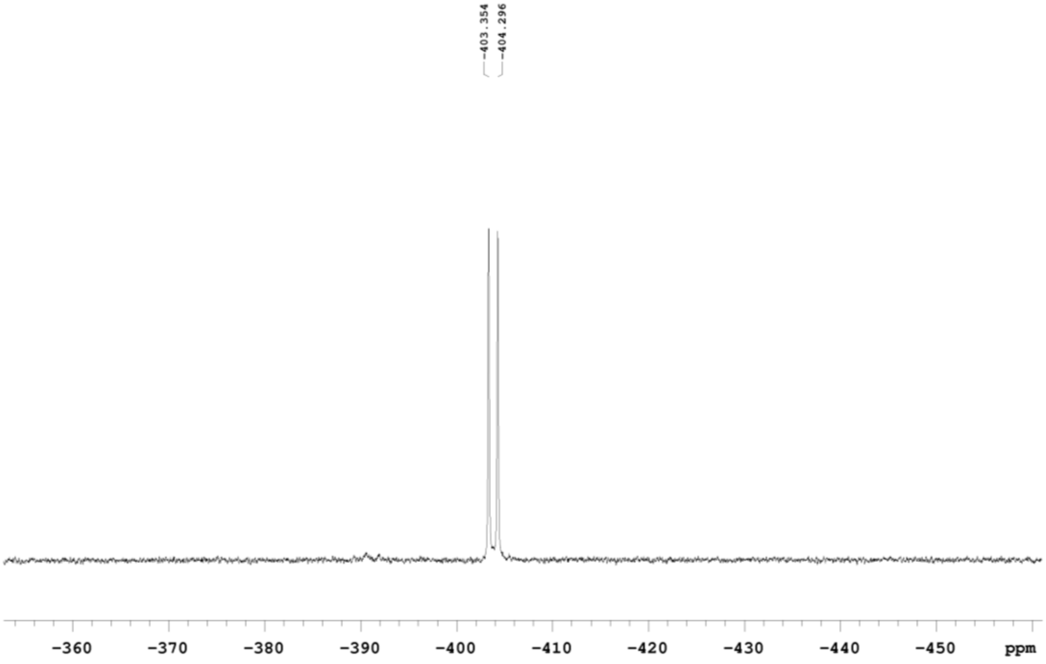

Figure S13. $^{31}P\{^{1}H\}$ NMR spectrum of [(ITr)Ag(η^2-PCO)] (**7**) in C_6D_6 at -80 °C in toluene-d_8.

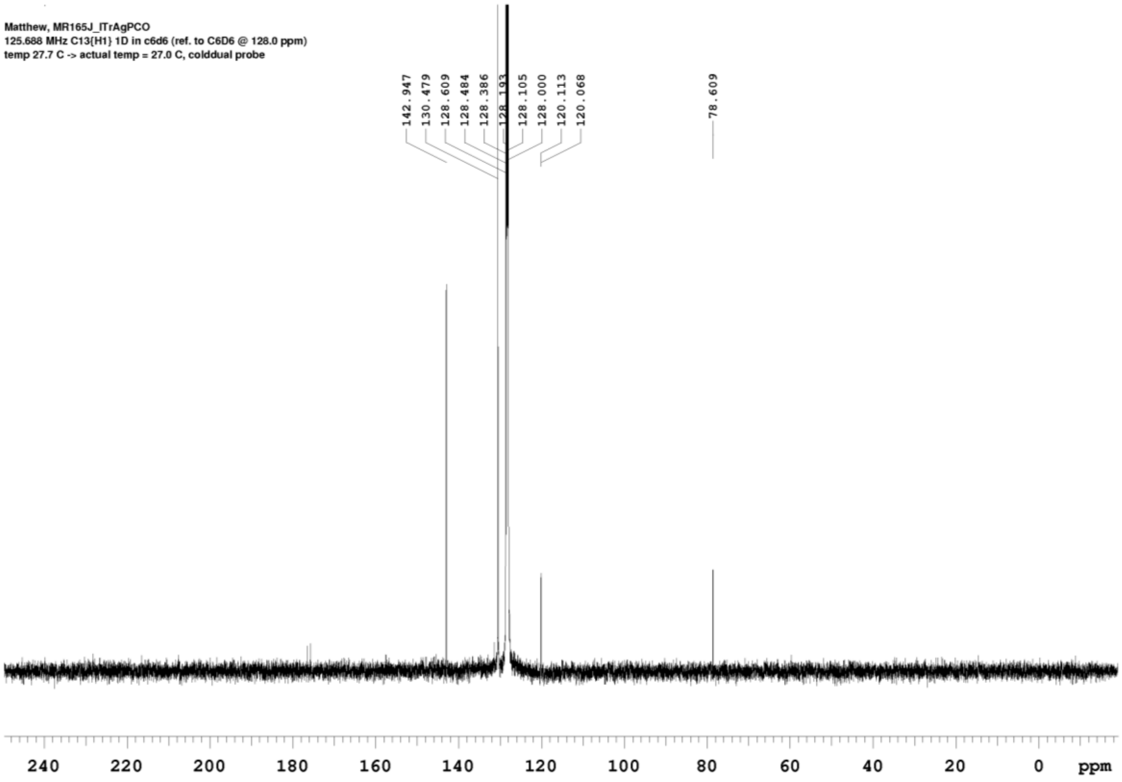

Figure S14. $^{13}C\{^{1}H\}$ NMR spectrum of [(ITr)Ag(η^2-PCO)] (**7**) in C_6D_6.

X-Ray Crystallographic Data

Table S1. Crystallographic Experimental Details for [(ITr)Ag(OTf)] (**1**).

A. Crystal Data

formula	$C_{42}H_{32}AgF_3N_2O_3S$
formula weight	809.62
crystal dimensions (mm)	0.15 × 0.13 × 0.09
crystal system	monoclinic
space group	$P2_1/m$ (No. 11)
unit cell parameters[a]	
a (Å)	9.4002 (2)
b (Å)	20.3414 (5)
c (Å)	9.8392 (2)
β (deg)	104.7623 (9)
V (Å^3)	1819.28 (7)
Z	2
ρ_{calcd} (g cm^{-3})	1.478
μ (mm^{-1})	5.466

B. Data Collection and Refinement Conditions

diffractometer	Bruker D8/APEX II CCD[b]
radiation (λ [Å])	Cu Kα (1.54178) (microfocus source)
temperature (°C)	–100
scan type	ω and ϕ scans (1.0°) (5 s exposures)
data collection 2θ limit (deg)	148.35
total data collected	13008 ($-11 \le h \le 11$, $-21 \le k \le 24$, $-12 \le l \le 12$)
independent reflections	3746 ($R_{int} = 0.0345$)
number of observed reflections (*NO*)	3578 [$F_o^2 \ge 2\sigma(F_o^2)$]
structure solution method	intrinsic phasing (*SHELXT-2014*[c])
refinement method	full-matrix least-squares on F^2 (*SHELXL–2014*[d])
absorption correction method	Gaussian integration (face-indexed)
range of transmission factors	0.7839–0.5087
data/restraints/parameters	3746 / 0 / 274
goodness-of-fit (S)[e] [all data]	1.070
final R indices[f]	
R_1 [$F_o^2 \ge 2\sigma(F_o^2)$]	0.0317
wR_2 [all data]	0.0856
largest difference peak and hole	1.541 and –0.841 e Å^{-3}

[a] Obtained from least-squares refinement of 9256 reflections with $8.70° < 2\theta < 146.64°$.

[b] Programs for diffractometer operation, data collection, data reduction and absorption correction were those supplied by Bruker.

[c] Sheldrick, G. M. *Acta Crystallogr.* **2015**, *A71*, 3–8. (*SHELXT-2014*)

[d] Sheldrick, G. M. *Acta Crystallogr.* **2015**, *C71*, 3–8. (*SHELXL-2014*)

[e] $S = [\Sigma w(F_o^2 - F_c^2)^2/(n - p)]^{1/2}$ (n = number of data; p = number of parameters varied; $w = [\sigma^2(F_o^2) + (0.0431P)^2 + 1.2090P]^{-1}$ where $P = [\mathrm{Max}(F_o^2, 0) + 2F_c^2]/3$).

[f] $R_1 = \Sigma||F_o| - |F_c||/\Sigma|F_o|$; $wR_2 = [\Sigma w(F_o^2 - F_c^2)^2/\Sigma w(F_o^4)]^{1/2}$.

Table S2. Crystallographic Experimental Details for [(ITr)Ag(PhF)][BAr$^F{}_4$] (**3**).

A. Crystal Data	
formula	$C_{79}H_{49}AgBF_{25}N_2$
formula weight	1619.88
crystal dimensions (mm)	0.43 × 0.36 × 0.25
crystal system	monoclinic
space group	$P2_1/n$ (an alternate setting of $P2_1/c$ [No. 14])
unit cell parameters[a]	
a (Å)	15.1650 (7)
b (Å)	26.0219 (12)
c (Å)	18.5838 (9)
β (deg)	101.2305 (6)
V (Å^3)	101.2305 (6)
Z	4
ρ_{calcd} (g cm^{-3})	1.496
μ (mm^{-1})	0.391
B. Data Collection and Refinement Conditions	
diffractometer	Bruker D8/APEX II CCD[b]
radiation (λ [Å])	graphite-monochromated Mo Kα (0.71073)
temperature (°C)	–100
scan type	ω scans (0.3°) (15 s exposures)
data collection 2θ limit (deg)	56.63
total data collected	64785 ($-20 \le h \le 20$, $-34 \le k \le 34$, $-24 \le l \le 24$)
independent reflections	17602 ($R_{\text{int}} = 0.0374$)
number of observed reflections (*NO*)	12524 [$F_o^2 \ge 2\sigma(F_o^2)$]
structure solution method	intrinsic phasing (*SHELXT-2014*[c])
refinement method	full-matrix least-squares on F^2 (*SHELXL–2014*[d])
absorption correction method	Gaussian integration (face-indexed)
range of transmission factors	0.9442–0.8955
data/restraints/parameters	17602 / 31[e] / 1006
goodness-of-fit (S)[f] [all data]	1.049
final R indices[g]	
R_1 [$F_o^2 \ge 2\sigma(F_o^2)$]	0.0572
wR_2 [all data]	0.1714
largest difference peak and hole	0.889 and –0.531 e Å^{-3}

[a] Obtained from least-squares refinement of 9804 reflections with 4.46° < 2θ < 43.52°.

[b] Programs for diffractometer operation, data collection, data reduction and absorption correction were those supplied by Bruker.

[c] Sheldrick, G. M. *Acta Crystallogr.* **2015**, *A71*, 3–8. (*SHELXT-2014*)

[d] Sheldrick, G. M. *Acta Crystallogr.* **2015**, *C71*, 3–8. (*SHELXL-2016*)

[e] The C–F distances within the disordered CF3 groups were restrained to be approximately equal by use of the *SHELXL* **SAME** instruction. Likewise, the C–F distances within the disordered coordinated fluorobenzene were also restrained to be approximately equal.

[f] $S = [\Sigma w(F_o^2 - F_c^2)^2/(n - p)]^{1/2}$ (n = number of data; p = number of parameters varied; $w = [\sigma^2(F_o^2) + (0.0857P)^2 + 5.3754P]^{-1}$ where $P = [\mathrm{Max}(F_o^2, 0) + 2F_c^2]/3$).

[g] $R_1 = \Sigma||F_o| - |F_c||/\Sigma|F_o|$; $wR_2 = [\Sigma w(F_o^2 - F_c^2)^2/\Sigma w(F_o^4)]^{1/2}$.

Table S3. Crystallographic Experimental Details for [(ITr)Ag(MesH)][BAr$^{\mathrm{F}}{}_{4}$]•1.5MesH (**4**).

A. Crystal Data

formula	$C_{95.5}H_{74}AgBF_{24}N_2$
formula weight	1824.24
crystal dimensions (mm)	0.46 × 0.28 × 0.03
crystal system	triclinic
space group	$P\bar{1}$ (No. 2)
unit cell parameters[a]	
a (Å)	13.0012 (3)
b (Å)	16.8587 (4)
c (Å)	20.2367 (5)
α (deg)	93.9117 (15)
β (deg)	100.4578 (16)
γ (deg)	99.6917 (14)
V (Å^3)	4277.23 (18)
Z	2
ρ_{calcd} (g cm^{-3})	1.416
μ (mm^{-1})	2.767

B. Data Collection and Refinement Conditions

diffractometer	Bruker D8/APEX II CCD[b]
radiation (λ [Å])	Cu Kα (1.54178) (microfocus source)
temperature (°C)	–100
scan type	ω and ϕ scans (1.0°) (5 s exposures)
data collection 2θ limit (deg)	148.07
total data collected	30571 ($-16 \leq h \leq 16$, $-21 \leq k \leq 20$, $-25 \leq l \leq 24$)
independent reflections	16677 ($R_{\mathrm{int}} = 0.0344$)
number of observed reflections (*NO*)	13630 [$F_o^2 \geq 2\sigma(F_o^2)$]
structure solution method	intrinsic phasing (*SHELXT-2014*[c])
refinement method	full-matrix least-squares on F^2 (*SHELXL–2014*[d])
absorption correction method	Gaussian integration (face-indexed)
range of transmission factors	0.9851–0.4537
data/restraints/parameters	16677 / 18[e] / 1151
goodness-of-fit (S)[f] [all data]	1.046
final R indices[g]	
R_1 [$F_o^2 \geq 2\sigma(F_o^2)$]	0.0581
wR_2 [all data]	0.1820
largest difference peak and hole	0.825 and –0.909 e Å^{-3}

[a] Obtained from least-squares refinement of 9851 reflections with 7.04° < 2θ < 145.70°.

[b] Programs for diffractometer operation, data collection, data reduction and absorption correction were those supplied by Bruker.

[c] Sheldrick, G. M. *Acta Crystallogr.* **2015**, *A71*, 3–8.

[d] Sheldrick, G. M. *Acta Crystallogr.* **2015**, *C71*, 3–8.

[e] (a) The $C_{aromatic}$–CH_3 bonds in the disordered solvent mesitylene molecules were constrained during refinement: d(C11S–C17S) = d(C13S–C18S) = d(C15S–C19S) = d(C21S–C27S) = d(C23S–C28S) = d(C25S–C29S) = d(C31S–C37S) = d(C33S–C38S) = d(C35S–C39S) = 1.52(1) Å. (b) Distances between the methyl carbons and the ortho carbons in one of the disordered solvent mesitylene molecules were constrained during refinement: d(C22S⋯C27S) = d(C26S⋯C27S) = d(C22S⋯C28S) = d(C24S⋯C28S) = d(C24S⋯C29S) = d(C26S⋯C29S) = 2.50(1) Å. (c) Methyl carbon positons for one of the disordered solvent mesitylene molecules were constrained to be coplanar with the aromatic ring carbons by defining the atoms C27S, C28S, C29S, C22S, C24S, C26S as vertices of a polyhedron with a volume to not exceed 0.01 Å^3 (*SHELXL-2014* FLAT instruction). (d) The ring carbons of the disordered solvent mesitylene molecules were modelled as idealized regular hexagons, with C–C bond distances of 1.390 Å and bond angles of 120.0º.

[f] $S = [\Sigma w(F_o^2 - F_c^2)^2/(n - p)]^{1/2}$ (n = number of data; p = number of parameters varied; $w = [\sigma^2(F_o^2) + (0.1181P)^2 + 1.3067P]^{-1}$ where $P = [\mathrm{Max}(F_o^2, 0) + 2F_c^2]/3$).

[g] $R_1 = \Sigma||F_o| - |F_c||/\Sigma|F_o|$; $wR_2 = [\Sigma w(F_o^2 - F_c^2)^2/\Sigma w(F_o^4)]^{1/2}$.

Table S4. Crystallographic Experimental Details for $[(\mathrm{ITr})\mathrm{Ag}(\mathrm{CH_2Cl_2})_{0.7}(\mathrm{toluene})_{0.3}][\mathrm{BAr^F}_4]\bullet\mathrm{CH_2Cl_2}$ (**5**).

A. Crystal Data	
formula	$C_{76.80}H_{49.80}AgBCl_{3.40}F_{24}N_2$
formula weight	1695.79
crystal dimensions (mm)	0.28 × 0.13 × 0.07
crystal system	monoclinic
space group	$P2_1/n$ (an alternate setting of $P2_1/c$ [No. 14])
unit cell parameters[a]	
a (Å)	15.3180 (3)
b (Å)	25.8009 (5)
c (Å)	18.7754 (4)
β (deg)	101.5004 (12)
V (Å^3)	7271.4 (3)
Z	4
ρ_{calcd} (g cm^{-3})	1.549
μ (mm^{-1})	4.329
B. Data Collection and Refinement Conditions	
diffractometer	Bruker D8/APEX II CCD[b]
radiation (λ [Å])	Cu Kα (1.54178) (microfocus source)
temperature (°C)	–100
scan type	ω and ϕ scans (1.0°) (5 s exposures)
data collection 2θ limit (deg)	145.11
total data collected	50317 ($-18 \le h \le 18$, $-31 \le k \le 31$, $-23 \le l \le 23$)
independent reflections	14382 ($R_{\mathrm{int}} = 0.0464$)
number of observed reflections (*NO*)	11638 [$F_o^2 \ge 2\sigma(F_o^2)$]
structure solution method	intrinsic phasing (*SHELXT-2014*[c])
refinement method	full-matrix least-squares on F^2 (*SHELXL–2014*[d])
absorption correction method	Gaussian integration (face-indexed)
range of transmission factors	1.0000–0.8010
data/restraints/parameters	14382 / 55[e] / 1062
goodness-of-fit (S)[f] [all data]	1.081
final R indices[g]	
R_1 [$F_o^2 \ge 2\sigma(F_o^2)$]	0.0689
wR_2 [all data]	0.2056
largest difference peak and hole	0.916 and –1.406 e Å^{-3}

[a] Obtained from least-squares refinement of 9852 reflections with $6.82° < 2\theta < 143.54°$.

[b] Programs for diffractometer operation, data collection, data reduction and absorption correction were those supplied by Bruker.

[c] Sheldrick, G. M. *Acta Crystallogr.* **2015**, *A71*, 3–8. (*SHELXT-2014*)

[d] Sheldrick, G. M. *Acta Crystallogr.* **2015**, *C71*, 3–8. (*SHELXL-2014*)

[e] The Cl–C distances within the coordinated dichloromethane was restrained to be approximately the same by use of the *SHELXL* **SAME** instruction. Likewise, the C–F distances within the CF_3 groups with carbon atoms C98 and C107 were also restrained. The coordinated toluene was constrained to be an idealized hexagon and the 1,3 interatomic distances involving the methyl group and the ortho-carbon atoms were restrained to be 2.50(1) Å. Finally, the Cl–C distances within the solvent dichloromethane molecules were restrained to be 1.80(2) Å, and the rigid-bond approximation (**RIGU**) was applied.

[f] $S = [\Sigma w(F_o^2 - F_c^2)^2/(n - p)]^{1/2}$ (n = number of data; p = number of parameters varied; $w = [\sigma^2(F_o^2) + (0.1126P)^2 + 7.3244P]^{-1}$ where $P = [\mathrm{Max}(F_o^2, 0) + 2F_c^2]/3$).

[g] $R_1 = \Sigma||F_o| - |F_c||/\Sigma|F_o|$; $wR_2 = [\Sigma w(F_o^2 - F_c^2)^2/\Sigma w(F_o^4)]^{1/2}$.

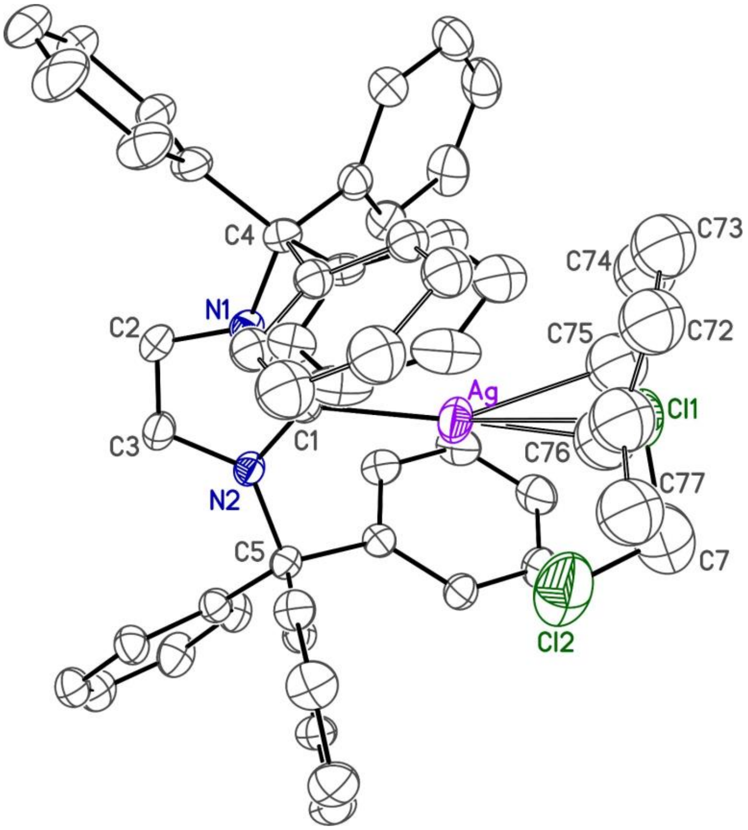

Figure S15. Molecular structure of $[(\mathrm{ITr})\mathrm{Ag}(\mathrm{CH_2Cl_2})_{0.7}(\mathrm{toluene})_{0.3}][\mathrm{BAr^F}_4]$ (**5**) with thermal ellipsoids plotted at the 30 % probability level. All hydrogen atoms and the $[\mathrm{BAr^F}]^-$ counterion were omitted for clarity.

Table S5. Crystallographic Experimental Details for [(ITr)Ag]$_2$[BAr$^F{}_4$]$_2$•hexane (**6**).

A. Crystal Data	
formula	$C_{158}H_{116}Ag_2B_2F_{48}N_4$
formula weight	3219.90
crystal dimensions (mm)	0.25 × 0.05 × 0.04
crystal system	triclinic
space group	$P\bar{1}$ (No. 2)
unit cell parameters[a]	
a (Å)	15.6902 (3)
b (Å)	16.2845 (4)
c (Å)	16.4921 (4)
α (deg)	117.7485 (13)
β (deg)	92.4871 (15)
γ (deg)	105.9078 (15)
V (Å^3)	3513.30 (15)
Z	1
ρ_{calcd} (g cm^{-3})	1.522
μ (mm^{-1})	3.284
B. Data Collection and Refinement Conditions	
diffractometer	Bruker D8/APEX II CCD[b]
radiation (λ [Å])	Cu Kα (1.54178) (microfocus source)
temperature (°C)	–100
scan type	ω and ϕ scans (1.0°) (5 / 5 / 15 s exposures)
data collection 2θ limit (deg)	145.24
total data collected	21964 ($-19 \le h \le 19$, $-20 \le k \le 20$, $-20 \le l \le 20$)
independent reflections	13276 (R_{int} = 0.0514)
number of observed reflections (*NO*)	9284 [$F_o^2 \ge 2\sigma(F_o^2)$]
structure solution method	intrinsic phasing (*SHELXT-2014*[c])
refinement method	full-matrix least-squares on F^2 (*SHELXL–2014*[d,e])
absorption correction method	Gaussian integration (face-indexed)
range of transmission factors	0.9787–0.6236
data/restraints/parameters	13276 / 118[f] / 1072
goodness-of-fit (*S*)[g] [all data]	1.023
final *R* indices[h]	
R_1 [$F_o^2 \ge 2\sigma(F_o^2)$]	0.0605
wR_2 [all data]	0.1720
largest difference peak and hole	0.592 and –1.316 e Å^{-3}

[a] Obtained from least-squares refinement of 7544 reflections with 5.98° < 2θ < 139.82°.

[b] Programs for diffractometer operation, data collection, data reduction and absorption correction

were those supplied by Bruker.

[c] Sheldrick, G. M. *Acta Crystallogr.* **2015**, *A71*, 3–8. (*SHELXT-2014/5*)

[d] Sheldrick, G. M. *Acta Crystallogr.* **2015**, *C71*, 3–8. (*SHELXL-2016/6*)

[e] Attempts to refine peaks of residual electron density as disordered or partial-occupancy solvent hexane carbon atoms were unsuccessful. The data were corrected for disordered electron density through use of the SQUEEZE procedure as implemented in *PLATON* (Spek, A. L. *Acta Crystallogr.* **2015**, *C71*, 9–18. *PLATON* - a multipurpose crystallographic tool. Utrecht University, Utrecht, The Netherlands). A total solvent-accessible void volume of 417 Å^3 with a total electron count of 110 (consistent with 2 molecules of solvent hexane) was found in the unit cell.

[f] The C–F distances within the disordered CF_3 groups were restrained to be approximately the same by use of the *SHELXL* **SADI** instruction. Likewise, the following pairs of distances involving the disordered aryl group were also restrained: B–C81A and B–C81B distances were restrained, the C83A–C87A and C83B–C87B, and the C85A–C88A and C85B–C88B. Finally, the atoms within the disordered bis(trifluoromethyl)phenyl groups were restrained to lie in approximately the same plane by use of the *SHELXL* **FLAT** instruction.

[g] $S = [\Sigma w(F_o^2 - F_c^2)^2/(n - p)]^{1/2}$ (n = number of data; p = number of parameters varied; $w = [\sigma^2(F_o^2) + (0.0845P)^2]^{-1}$ where $P = [\mathrm{Max}(F_o^2, 0) + 2F_c^2]/3$).

[h] $R_1 = \Sigma||F_o| - |F_c||/\Sigma|F_o|$; $wR_2 = [\Sigma w(F_o^2 - F_c^2)^2/\Sigma w(F_o^4)]^{1/2}$.

Table S6. Crystallographic Experimental Details for [(ITr)Ag(PCO)]•2C_4H_8O (**7**).

A. Crystal Data

formula	$C_{50}H_{48}AgN_2O_3P$
formula weight	863.74
crystal dimensions (mm)	0.22 × 0.16 × 0.04
crystal system	triclinic
space group	$P\bar{1}$ (No. 2)
unit cell parameters[a]	
a (Å)	11.15213 (16)
b (Å)	11.75148 (17)
c (Å)	16.7352 (3)
α (deg)	83.7416 (11)
β (deg)	85.9962 (8)
γ (deg)	71.1237 (9)
V (Å^3)	2061.50 (5)
Z	2
ρ_{calcd} (g cm^{-3})	1.391
μ (mm^{-1})	4.644

B. Data Collection and Refinement Conditions

diffractometer	Bruker D8/APEX II CCD[b]
radiation (λ [Å])	Cu Kα (1.54178) (microfocus source)
temperature (°C)	–100
scan type	ω and ϕ scans (1.0°) (5 s exposures)
data collection 2θ limit (deg)	147.87
total data collected	14722 ($-13 \le h \le 13$, $-14 \le k \le 14$, $-20 \le l \le 20$)
independent reflections	8024 ($R_{\text{int}} = 0.0287$)
number of observed reflections (*NO*)	7411 [$F_o^2 \ge 2\sigma(F_o^2)$]
structure solution method	intrinsic phasing (*SHELXT-2014*[c])
refinement method	full-matrix least-squares on F^2 (*SHELXL–2014*[d])
absorption correction method	Gaussian integration (face-indexed)
range of transmission factors	0.8910–0.4758
data/restraints/parameters	8024 / 0 / 514
goodness-of-fit (S)[e] [all data]	1.058
final R indices[f]	
R_1 [$F_o^2 \ge 2\sigma(F_o^2)$]	0.0308
wR_2 [all data]	0.0844
largest difference peak and hole	0.774 and –0.720 e Å^{-3}

[a] Obtained from least-squares refinement of 9368 reflections with 8.38° < 2θ < 147.02°.

[b] Programs for diffractometer operation, data collection, data reduction and absorption correction were those supplied by Bruker.

[c] Sheldrick, G. M. *Acta Crystallogr.* **2015**, *A71*, 3–8.

[d] Sheldrick, G. M. *Acta Crystallogr.* **2015**, *C71*, 3–8.

[e] $S = [\Sigma w(F_o^2 - F_c^2)^2/(n - p)]^{1/2}$ (n = number of data; p = number of parameters varied; $w = [\sigma^2(F_o^2) + (0.0469P)^2 + 0.5798P]^{-1}$ where $P = [\mathrm{Max}(F_o^2, 0) + 2F_c^2]/3$).

[f] $R_1 = \Sigma||F_o| - |F_c||/\Sigma|F_o|$; $wR_2 = [\Sigma w(F_o^2 - F_c^2)^2/\Sigma w(F_o^4)]^{1/2}$.

Computational Studies

The following calculations (except methyl ion affinity calculations – see below) were carried out using the Gaussian 09, Rev. D.01 software package.[7] Input structures were optimized using the B3LYP[8] functional and 6-31G(d,p)[9] basis set in the gas phase. An effective core potential (ECP) LANL2DZ[10] was used for silver. The optimized geometries were confirmed to be minima on the potential energy surface using frequency analysis.

Optimization Results for [(ITr)Ag]$^+$:

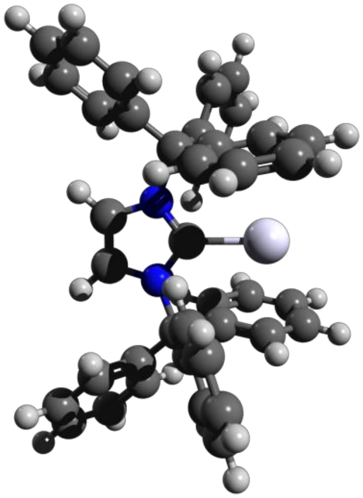

Figure S16. Optimized geometry of [(ITr)Ag]$^+$.

Ag	-0.00014	2.00106	0.00007
N	1.08914	-1.00870	-0.07735
N	-1.08904	-1.00872	0.07733
C	0.00005	-0.18008	-0.00003
C	0.67941	-2.34996	-0.04967
H	1.36428	-3.17429	-0.10544
C	-0.67928	-2.34998	0.04955
H	-1.36414	-3.17431	0.10528
C	2.52207	-0.47574	-0.14256
C	-2.52199	-0.47582	0.14251
C	2.95559	0.04678	1.25304
C	4.28892	0.47687	1.41051
H	4.97285	0.42540	0.56976
C	4.74865	0.95405	2.63936

H	5.77848	1.28102	2.73606
C	3.88974	0.99582	3.74606
H	4.24881	1.35718	4.70358
C	2.57317	0.55295	3.60655
H	1.90240	0.56182	4.45949
C	2.10709	0.08316	2.36880
H	1.08484	-0.26333	2.29523
C	3.49080	-1.63379	-0.51805
C	4.22295	-1.67260	-1.71491
H	4.12823	-0.88193	-2.44638
C	5.11489	-2.72256	-1.97643
H	5.67281	-2.72588	-2.90679
C	5.29357	-3.74925	-1.04783
H	5.98377	-4.56038	-1.25277
C	4.58880	-3.70988	0.16234
H	4.73665	-4.48656	0.90521
C	3.71044	-2.65814	0.42839
H	3.20937	-2.61915	1.39002
C	2.46851	0.65618	-1.20398
C	2.03746	0.35653	-2.51059
H	1.80834	-0.66953	-2.77758
C	1.87782	1.36245	-3.46923
H	1.55825	1.10086	-4.47253
C	2.12087	2.70129	-3.13820
H	1.99622	3.48148	-3.88114
C	2.53904	3.02006	-1.84112
H	2.75620	4.04959	-1.57445
C	2.71685	2.00542	-0.88131
H	3.08231	2.26989	0.10343
C	-2.46854	0.65609	1.20397
C	-2.71702	2.00533	0.88134
H	-3.08257	2.26978	-0.10336
C	-2.53932	3.01995	1.84119
H	-2.75659	4.04947	1.57455
C	-2.12112	2.70118	3.13826
H	-1.99655	3.48137	3.88122
C	-1.87792	1.36236	3.46925
H	-1.55833	1.10077	4.47253
C	-2.03745	0.35645	2.51058
H	-1.80826	-0.66960	2.77754
C	-3.49064	-1.63392	0.51800
C	-3.71024	-2.65825	-0.42848
H	-3.20920	-2.61919	-1.39012
C	-4.58850	-3.71009	-0.16244
H	-4.73634	-4.48673	-0.90534
C	-5.29321	-3.74956	1.04776

H	-5.98332	-4.56076	1.25273
C	-5.11456	-2.72290	1.97641
H	-5.67243	-2.72633	2.90680
C	-4.22273	-1.67285	1.71489
H	-4.12804	-0.88220	2.44639
C	-2.95556	0.04671	-1.25307
C	-2.10705	0.08326	-2.36883
H	-1.08476	-0.26312	-2.29529
C	-2.57318	0.55308	-3.60655
H	-1.90241	0.56208	-4.45949
C	-3.88980	0.99580	-3.74605
H	-4.24890	1.35719	-4.70354
C	-4.74871	0.95389	-2.63935
H	-5.77857	1.28076	-2.73604
C	-4.28893	0.47667	-1.41053
H	-4.97287	0.42506	-0.56980

Optimization Results for [(ITr)Ag(PCO)]:

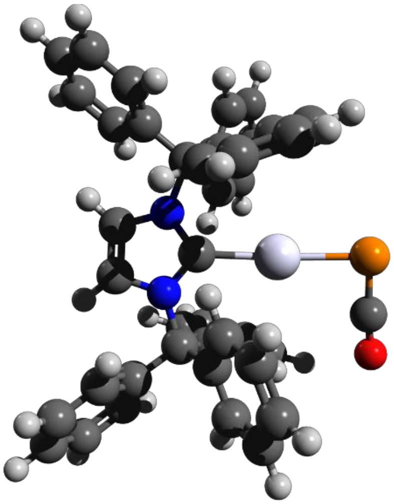

Figure S17. Optimized geometry of [(ITr)Ag(PCO)].

Ag	0.07512	-1.74380	-0.14628
P	0.17430	-4.24756	-0.29342
O	2.90388	-4.36492	0.64909
N	-1.26767	1.19128	-0.01733
N	0.90263	1.37734	-0.00518
C	-0.10955	0.44204	-0.04934
C	-0.97436	2.56176	0.04520

H	-1.72885	3.32382	0.06931
C	0.37907	2.67695	0.06167
H	0.99354	3.55507	0.10916
C	-2.65834	0.58375	-0.10802
C	2.37390	1.01026	0.12967
C	1.76783	-4.26759	0.25920
C	-2.65724	-0.27320	-1.40297
C	-2.20966	0.31944	-2.60244
H	-1.87320	1.35148	-2.59841
C	-2.18367	-0.40238	-3.79739
H	-1.83767	0.07743	-4.70772
C	-2.59585	-1.74150	-3.81973
H	-2.56794	-2.30794	-4.74467
C	-3.02643	-2.34353	-2.63659
H	-3.32228	-3.38704	-2.63110
C	-3.05674	-1.61692	-1.43716
H	-3.37103	-2.11754	-0.53159
C	-3.70569	1.73992	-0.17056
C	-4.48935	2.00642	-1.30292
H	-4.37599	1.40859	-2.19704
C	-5.44055	3.03725	-1.29141
H	-6.03830	3.21830	-2.17903
C	-5.62397	3.82002	-0.15037
H	-6.36032	4.61711	-0.14348
C	-4.85725	3.55587	0.99260
H	-4.99943	4.14461	1.89323
C	-3.91992	2.52169	0.98468
H	-3.35642	2.30716	1.88649
C	-2.98508	-0.23211	1.17202
C	-2.08018	-0.42697	2.22528
H	-1.07768	-0.02563	2.17399
C	-2.45548	-1.14934	3.36757
H	-1.73137	-1.29252	4.16280
C	-3.73924	-1.68560	3.47823
H	-4.02456	-2.25070	4.35945
C	-4.65830	-1.48050	2.44117
H	-5.66488	-1.87929	2.51659
C	-4.28770	-0.75459	1.30782
H	-5.01918	-0.58202	0.52539
C	2.86773	0.22351	-1.11225
C	2.08130	-0.00301	-2.25133
H	1.05015	0.32125	-2.28111
C	2.61401	-0.65988	-3.36998
H	1.98075	-0.83315	-4.23394
C	3.93938	-1.09737	-3.37073
H	4.34660	-1.61478	-4.23306

C	4.73987	-0.85792	-2.24670
H	5.77499	-1.18324	-2.23421
C	4.21277	-0.19613	-1.13663
H	4.85352	0.00335	-0.28456
C	2.46605	0.21581	1.46024
C	2.00120	0.83114	2.64196
H	1.61984	1.84697	2.60671
C	2.01580	0.15101	3.86167
H	1.65954	0.64892	4.75846
C	2.48316	-1.16925	3.92556
H	2.48963	-1.70205	4.87105
C	2.92531	-1.79652	2.75989
H	3.25578	-2.82880	2.77208
C	2.91644	-1.10965	1.53611
H	3.24531	-1.63722	0.65149
C	3.22267	2.31880	0.15095
C	3.22790	3.14369	-0.99376
H	2.62837	2.86727	-1.85467
C	4.00832	4.29943	-1.04599
H	3.99066	4.91941	-1.93669
C	4.82651	4.64641	0.03781
H	5.44171	5.53935	-0.00460
C	4.85345	3.82252	1.16415
H	5.49531	4.06778	2.00429
C	4.05822	2.66849	1.22186
H	4.10447	2.04204	2.10248

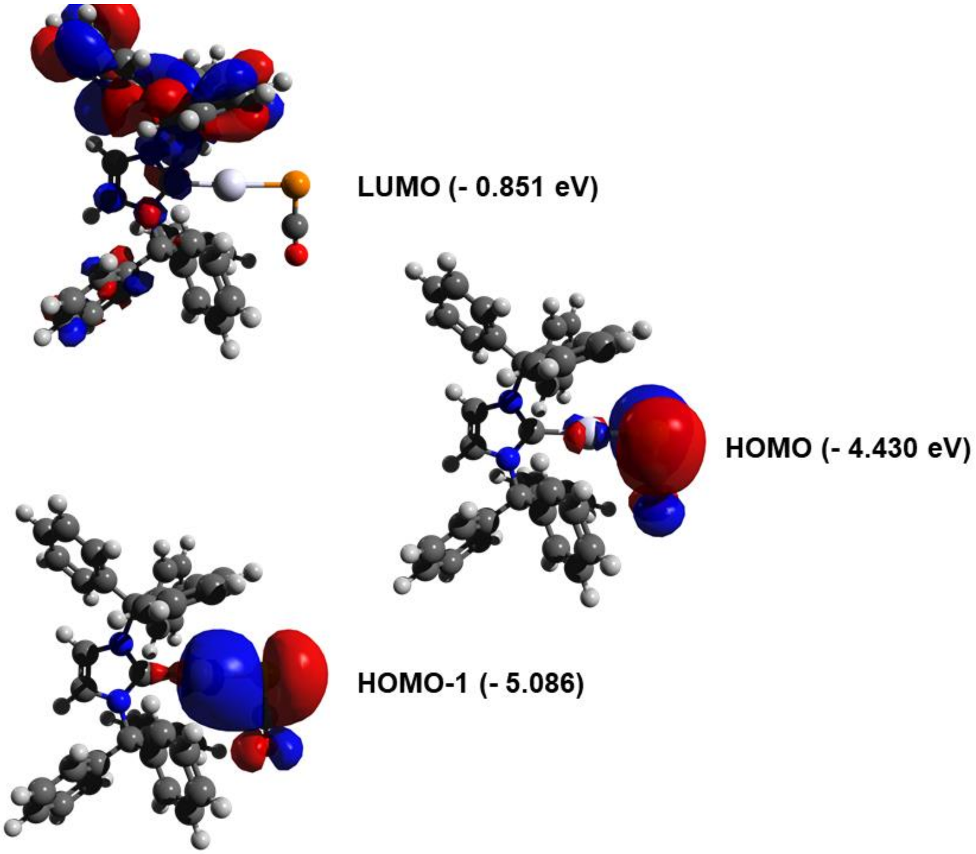

Figure S18. Selected molecular orbitals of [(ITr)Ag(PCO)] demonstrating the η^2 -PCO bonding (HOMO-1).

Methyl Ion Affinity and $[(\mathrm{IMe})\mathrm{Ag}]^+$ Arene Coordination

The following calculations were carried out using the ORCA 4.0.0.2 software package.[11] Input structures were optimized using the (RI-)BP86[12] functional and the def2-SV(P)[13] basis set in the gas phase. The optimized geometries were confirmed to be minima on the potential energy surface using frequency analysis. A truncated model was used in place of the ITr ligand, IMe $[(\mathrm{HCNCH_3})_2\mathrm{C}:]$. The enthalpy of fluorobenzene coordination to $[(\mathrm{IMe})\mathrm{Ag}]^+$ was calculated by determining the reaction enthalpy of: $[(\mathrm{IMe})\mathrm{Ag}]^+ + \mathrm{PhF} \rightarrow [(\mathrm{IMe})\mathrm{Ag}(\mathrm{PhF})]^+$. The methyl ion affinity (MIA) was calculated as described in the literature[14] referenced to the MIA of $\mathrm{SiMe_3}^+$ calculated at the G3 level ($\Delta_r H$ =1000 kJ/mol)[14] according to the following set of equations:

$$\mathrm{SiMe_4} \xrightarrow{\text{G3}} \overset{\oplus}{\mathrm{SiMe_3}} + \overset{\ominus}{:\mathrm{CH_3}} \quad \Delta_r H = 1000\ \text{kJ/mol}$$

$$[(\mathrm{IMe})\mathrm{Ag}]^{\oplus} + \mathrm{SiMe_4} \xrightarrow{\text{DFT}} [(\mathrm{IMe})\mathrm{Ag}(\mathrm{CH_3})] + \overset{\oplus}{\mathrm{SiMe_3}}$$

$$[(\mathrm{IMe})\mathrm{Ag}]^{\oplus} + \overset{\ominus}{:\mathrm{CH_3}} \longrightarrow [(\mathrm{IMe})\mathrm{Ag}(\mathrm{CH_3})]$$

$$\begin{aligned} -\,\mathrm{MIA} = \Delta_r H &= H_{[(\mathrm{IMe})\mathrm{Ag}(\mathrm{CH3})]} - H_{[(\mathrm{IMe})\mathrm{Ag}]+} - H_{\mathrm{SiMe4}} + H_{\mathrm{SiMe3+}} - 1000\ \text{kJ/mol} \\ &= -1290117 + 1184968 + 1178364 - 1072995 - 1000\ \text{kJ/mol} \\ &= -\,780\ \text{kJ/mol} \end{aligned}$$

Optimization Results for $\mathrm{SiMe_4}$:

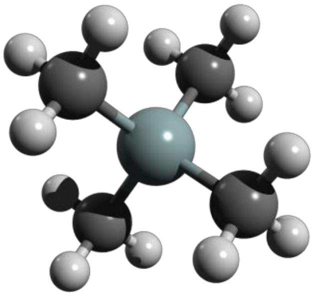

Figure S19. Optimized geometry of $\mathrm{SiMe_4}$.

Si	-2.22284385441402	1.25734300349353	0.00001455117658
C	-1.58994756464297	2.15369128717343	-1.55561996185743
H	-1.95163483481610	3.20625961973867	-1.59137055113801
H	-0.47651819008375	2.17917509588886	-1.58635825214712
H	-1.94170380319019	1.64754996641574	-2.48340905129183
C	-1.59176532713504	-0.53838670965090	0.00016458771405
H	-0.47830970044451	-0.57916095757411	0.00019646415265
H	-1.94916298581282	-1.09225616808289	0.89840178299072
H	-1.94909524354777	-1.09235080306572	-0.89804333234404
C	-1.59017068746119	2.15394448693463	1.55559006038076
H	-1.95184785775399	3.20652615887722	1.59108015318464
H	-1.94205811133670	1.64797633693315	2.48342187274814
H	-0.47674506594987	2.17943669515971	1.58649141163865
C	-4.12600307794326	1.25745963063744	-0.00011801163814
H	-4.53241894257055	0.73833412848567	-0.89817574315521
H	-4.53254748881630	0.73842634016301	0.89793485116562
H	-4.53322726408097	2.29403188847256	-0.00020083158002

Optimization Results for $SiMe_3^+$:

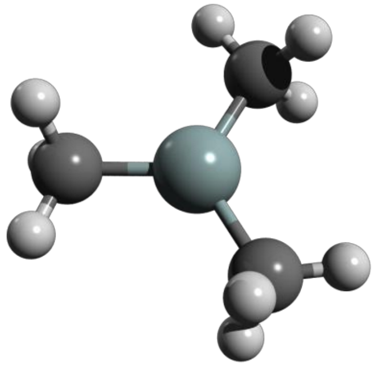

Figure S20. Optimized geometry of $SiMe_3^+$.

Si	-1.05647726911293	-0.77199648987669	-1.15751297336041
C	-1.95219940140758	-2.38748137996604	-1.13664416612041
H	-2.44936256694477	-2.52702548174693	-0.14527308371766
H	-2.77951596414543	-2.37456577528788	-1.88816189447330

H	-1.29070991851030	-3.25699833176739	-1.33637712373384
C	0.76357560781992	-0.72972724206425	-1.47080130286891
H	0.98538811881500	-1.19707610128291	-2.46177400852117
H	1.18917547332812	0.29591372331777	-1.45078770287964
H	1.29340341310201	-1.36154906137894	-0.71634663099190
C	-1.97598846850852	0.80163543478008	-0.85719074242584
H	-1.54706108192203	1.31717793387869	0.03749195159970
H	-1.81740807782173	1.50322606051733	-1.71328974956964
H	-3.06581986469175	0.65246671087717	-0.70233257293699

Optimization Results for [(IMe)Ag]$^+$:

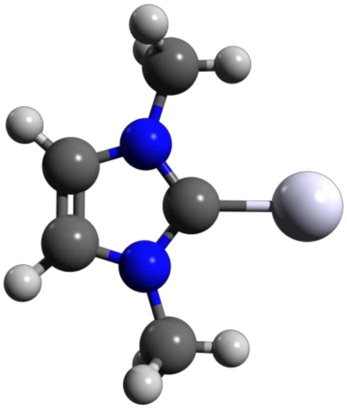

Figure S21. Optimized geometry of [(IMe)Ag]$^+$.

N	12.34717541491880	14.57998038378339	4.33949300919307
N	11.02085919581708	14.48633191385261	2.61389096097488
C	11.19138929768422	14.01857325373042	3.88330735911093
C	12.90020760283501	15.39590606951380	3.36182042298855
H	13.83469112915899	15.94796186105310	3.51687989643341
C	12.06410906391473	15.33704842722733	2.27409985869981
H	12.12736396005933	15.82678912281348	1.29515486251498
Ag	9.94671633009828	12.71554501077494	4.91529927057813
C	12.94564740221464	14.36618254050899	5.65862438534637
H	12.27864770953201	13.70781473611543	6.25097141545586
H	13.93781496573478	13.87933058046654	5.55332921496169
H	13.06043669137664	15.33607128702727	6.18592670078380
C	9.91703113960460	14.14677670098978	1.71280817294381
H	10.29572103095408	13.56881635530578	0.84349438992096
H	9.17835238229648	13.53235045508486	2.26643443578410
H	9.42183668380033	15.07352130175225	1.35646564430967

Optimization Results for [(IMe)Ag(CH_3)]:

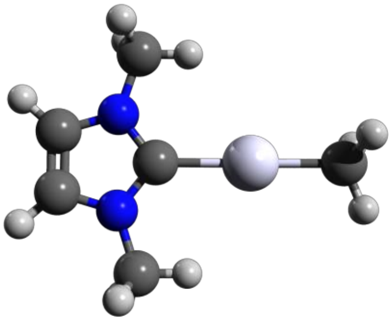

Figure S22. Optimized geometry of [(IMe)Ag(CH_3)].

N	12.42146087642418	14.50996364307593	4.26795052713000
N	11.06967560822251	14.48797840512656	2.58418692526994
C	11.21540514626492	14.00153062724768	3.85820363954429
C	13.01059185371881	15.29132766598825	3.27995680794187
H	13.98072087141816	15.78393788314097	3.41348502919255
C	12.15159489943572	15.27753993998963	2.20970582451574
H	12.22290376976096	15.75784196096542	1.22680617638633
Ag	9.88212694468616	12.76001747504974	4.94655613078518
C	8.57386198615928	11.54026547593668	6.03130073548379
H	9.05675674138706	10.57542886523513	6.31147048176453
H	8.24492823020685	12.03682063116051	6.97353002201173
H	7.65742338487787	11.29672029617248	5.44484251545638
C	13.00877171884191	14.25495150751199	5.57880325711367
H	13.98487439278556	13.73369153984054	5.47290948155522
H	13.15806775380893	15.20829535544660	6.13053753999611
H	12.30653712367088	13.60829307825709	6.14457289311121
C	9.91488099486169	14.21125922017981	1.73652488126459
H	10.23194669585213	13.70115326965335	0.80130463345017
H	9.23035027593932	13.54782690277652	2.30524646553572
H	9.38512073167714	15.15415625724513	1.48010603249097

Optimization Results for $[(IMe)Cu]^+$

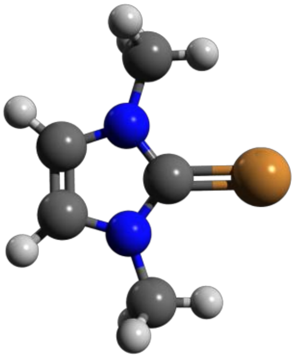

Figure S23. Optimized geometry of $[(IMe)Cu]^+$.

N	12.34338292500771	14.58186281522544	4.34176032809880
N	11.02401947653099	14.47690974306949	2.61260009052661
C	11.18557349562391	14.01551648874571	3.88834797792119
C	12.90116353834806	15.38918447312189	3.36147065816341
H	13.83765789442397	15.93855076184891	3.51417962898884
C	12.06826819460897	15.32370184735086	2.27058855438244
H	12.13576837915969	15.80766488523913	1.28897863211556
Cu	10.05828118325499	12.84978578021253	4.82641572739601
C	12.92759102938313	14.36205359687272	5.66540418461964
H	12.23068157157271	13.73261847525655	6.25546032562655
H	13.90342195040776	13.83995211541904	5.57515586467360
H	13.07029289492543	15.33140893636348	6.18691268210561
C	9.91098563069902	14.13663642910128	1.72496201666323
H	10.28975313253454	13.63971789300578	0.80736563433348
H	9.23354045489736	13.44156165806204	2.26170873133701
H	9.34761824862177	15.05187410110515	1.44668896304803

Optimization Results for [(IMe)Cu(CH3)]:

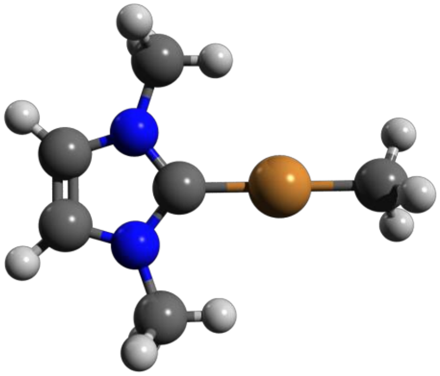

Figure S24. Optimized geometry of [(IMe)Cu(CH_3)].

N	12.37527306140366	14.47314458410580	4.30960232812491
N	11.02461043030096	14.43908152611204	2.62172471273524
C	11.16679262387981	13.95679885141699	3.90240282097414
C	12.96347004775824	15.24959698519391	3.31807415776416
H	13.93245684844754	15.74523666303809	3.44901536072058
C	12.10569922670912	15.22832046785972	2.24608605782123
H	12.17906578223563	15.70429841934783	1.26117397688818
Cu	9.96596136402110	12.83613446125445	4.88630808415257
C	8.75654148607234	11.70953971914681	5.87707339272921
H	8.34050847784137	10.88279870623124	5.25036519353223
H	9.25574221872816	11.22662839528505	6.75273652864157
H	7.88214873681516	12.27661616798857	6.28034391509054
C	12.94822577929313	14.21865852198428	5.62535606584929
H	13.92001307772587	13.68567883309150	5.53547419553288
H	13.10021041346820	15.17074022304944	6.17917940957513
H	12.22881097823767	13.58064133706145	6.18059730613616
C	9.86754640488649	14.14926188832289	1.78382511157765
H	10.17825783475844	13.63332134754833	0.84921354391119
H	9.19505999336084	13.48472802862470	2.36649545939475
H	9.32560521405627	15.08477487333694	1.52395237884841

Optimization Results for [(IMe)Au]$^+$:

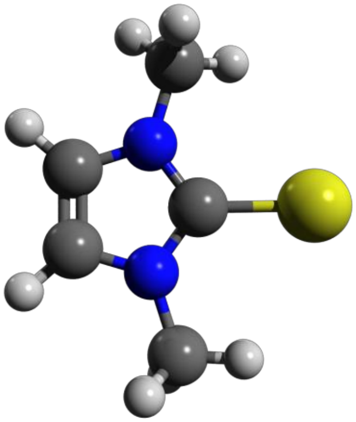

Figure S25. Optimized geometry of [(ITr)Au]$^+$.

N	12.36780202688278	14.54318522030362	4.33450444894247
N	11.00217709465295	14.49658905374117	2.61901862051683
C	11.18569666812386	14.03745758651996	3.88724735825783
C	12.93185764168926	15.33038025500500	3.34004459053240
H	13.88992685288992	15.84516811716394	3.47860620384492
C	12.07812543560663	15.29929073281136	2.26462100337640
H	12.14987663106415	15.77303635258488	1.27854121189436
Au	9.96047436155101	12.86606109630919	4.90274207012982
C	12.94092522621282	14.35899065034247	5.67275320535479
H	12.60585925723553	13.38573607556257	6.08301377252148
H	14.04669885044681	14.35589194388238	5.59263133861476
H	12.61677403901765	15.18062070127863	6.34695233976952
C	9.88614154804503	14.17180818039913	1.72277843406222
H	10.22425688456875	13.46547238765386	0.93521139015223
H	9.07310486747194	13.70526387148591	2.31305606685748
H	9.50830261454089	15.10404777495597	1.25627794517250

Optimization Results for [(IMe)Au(CH_3)]:

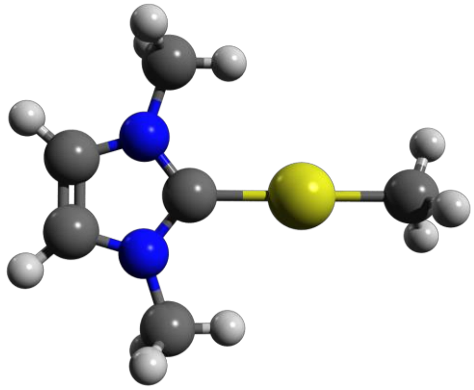

Figure S26. Optimized geometry of [(IMe)Au(CH_3)].

N	12.41330288038378	14.50824686068599	4.27907817932180
N	11.06200361746694	14.47522837346978	2.58868006591443
C	11.20779725107838	13.99565663138784	3.86718857427553
C	13.00090842932520	15.28513831599886	3.28679000094924
H	13.96982732832676	15.78001693677656	3.41976643134623
C	12.14430698865204	15.26461127331993	2.21533608204531
H	12.21657279159946	15.74064286565573	1.23052579474705
Au	9.89846351519900	12.77521643253297	4.93932999817999
C	8.59800085886088	11.56137381445941	6.00946764491445
H	8.19405300462982	10.73693269502302	5.37575628386933
H	9.10618507782793	11.09275429960777	6.88471280790313
H	7.72821368093645	12.14146693821940	6.39864758830291
C	13.00005510399599	14.26118404964753	5.59144354525478
H	13.97582510499617	13.73872021772830	5.48842941617526
H	13.14932147211204	15.21842564206264	6.13640112136101
H	12.29613815520814	13.61859056303303	6.15948195417862
C	9.91074891859381	14.19375858018809	1.73807966819963
H	10.23418203446782	13.68867874628579	0.80233121231254
H	9.22980206486692	13.52478456379317	2.30413913200953
H	9.37629172147246	15.13457220012419	1.48341449873922

Optimization Results for Ph_3C^+:

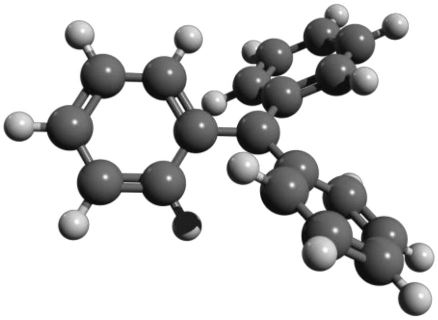

Figure S27. Optimized geometry of Ph_3C^+.

C	4.82417217933106	0.19575065749989	0.00258059438519
C	5.55441359108442	-0.72759139379502	0.81441876067719
C	5.55657493496584	1.11956565403515	-0.80677859351205
C	6.95198945306767	-0.71382216874897	0.82359455233862
H	5.00725176517289	-1.41306559261853	1.48091881003446
C	6.95417898557881	1.10682399045874	-0.81110410176767
H	5.01117294386738	1.80460109251681	-1.47518036780925
C	7.65428722127780	0.19677096766738	0.00749076878358
H	7.50410348147037	-1.40927020259034	1.47644458916797
H	7.50807002882128	1.80265962091460	-1.46203067985650
H	8.75772473995990	0.19721375026680	0.00944685359161
C	2.64028997236667	-1.05310451645612	0.17347459766586
C	1.38514984167361	-1.07803229842750	0.85865895103745
C	3.16264321306541	-2.28211100444142	-0.33823083230631
C	0.69514379974379	-2.28086405162859	1.03265797138284
H	0.99195651078969	-0.14997983364621	1.30230091522203
C	2.45137304889967	-3.47510869661667	-0.18188756690154
H	4.10346834110800	-2.27443664306165	-0.91064366489369
C	1.22214120028058	-3.47897323538017	0.50854241669072
H	-0.25668056250475	-2.29239647219619	1.58734990993876
H	2.84807253633160	-4.41047815759995	-0.60790976446830
H	0.66977990082986	-4.42431146954567	0.63889119836317
C	2.64017091817551	1.44343687302890	-0.17553365360286
C	3.16020872527845	2.67269449801588	0.33791521444320
C	1.38726258392771	1.46773259261221	-0.86482276742258
C	2.44884753824897	3.86533411597455	0.17929490730719
H	4.09916588968883	2.66548311398527	0.91340097228508
C	0.69721849944380	2.67022194957901	-1.04101223373767

H	0.99596780939529	0.53951471371955	-1.30978882392712
C	1.22188414438295	3.86858740403559	-0.51514869319545
H	2.84371000907802	4.80087846215950	0.60663961035831
H	-0.25281248092236	2.68129664795619	-1.59880084162418
H	0.66945490213036	4.81363303377309	-0.64729998053105
C	3.36864433399093	0.19534659855385	0.00015097188298

Optimization Results for Ph_3CCH_3:

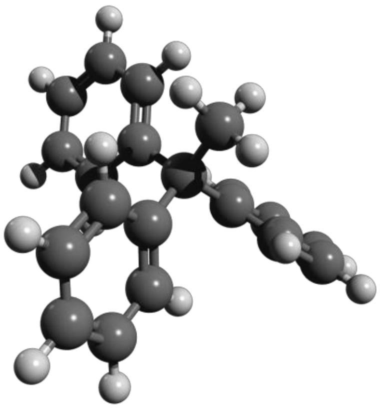

Figure S28. Optimized geometry of Ph_3CCH_3.

C	4.34443114082295	0.44948339572220	-0.03160181147922
C	4.70115912789472	1.27154429690750	-1.30664384805384
H	4.18279123100979	2.25330577102545	-1.30310948213333
H	5.79277877137757	1.45706784867722	-1.39170716364544
H	4.37535715929246	0.72900788710600	-2.21868576179260
C	2.79566360001135	0.45779854113114	0.07201510904072
C	2.02381988972165	-0.08753127943931	-0.98303569738276
C	2.10449932647642	1.04630429477611	1.15132254794863
C	0.62130483413595	-0.04799792681946	-0.95834402617829
H	2.52833111206874	-0.56655955105931	-1.83892374186231
C	0.69712513616743	1.08952162982438	1.17904364954301
H	2.67001042589052	1.48249265966490	1.98884060036801
C	-0.05209044023836	0.54426658238316	0.12579198985051
H	0.05005579136041	-0.48456716862297	-1.79551310791315
H	0.18704448166619	1.55738081956063	2.03852957717677
H	-1.15492234105322	0.57916997359420	0.14649476675314
C	4.98739925186757	1.08272192138484	1.23037650852984
C	5.13042048841087	0.32210137491321	2.41426982444033
C	5.42062524631068	2.42650534606122	1.26060390163617

C	5.68045646396420	0.87951746060457	3.57967723935567
H	4.80768246627967	-0.73126467426804	2.42280098019728
C	5.97576322471855	2.98868276461329	2.42532671574821
H	5.32485627235141	3.06093239919565	0.36648068630620
C	6.10936592729148	2.21845481673339	3.59119032472993
H	5.78145555601358	0.25743033327056	4.48545130098076
H	6.30868680907477	4.04024813620527	2.41461773102816
H	6.54809240249548	2.65648600093814	4.50348492758073
C	4.90065542539502	-0.99331429689385	-0.17991235810792
C	6.23328053967388	-1.19193769454146	-0.61049020263736
C	4.14447407480613	-2.13761009828906	0.15576655225115
C	6.78144510387440	-2.47978947474535	-0.71970154625308
H	6.86763656667836	-0.32507520569700	-0.85460503915273
C	4.69150532730551	-3.43013232198269	0.05207668707348
H	3.10669600142145	-2.02205079482701	0.50581838419891
C	6.01091809281457	-3.60916731575699	-0.39162056121702
H	7.82283284784855	-2.60019507752221	-1.06284942266208
H	4.07384821616090	-4.30335253962213	0.32238653631720
H	6.43954444863840	-4.62187883420621	-0.47862277058369

Optimization Results for $[MeZn]^+$:

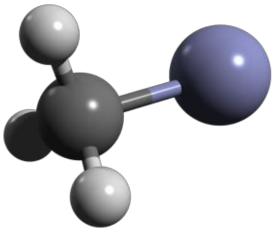

Figure S29. Optimized geometry of $[MeZn]^+$.

Zn	3.60768643986796	0.29619728566102	0.00011653045642
C	5.59024253421081	0.29638370726594	-0.00006872519779
H	5.86940112236242	-0.20783043893263	0.94854324004319
H	5.86968938552245	-0.27261341608054	-0.91122761057364
H	5.86898051803637	1.36986286208620	-0.03736343472818

Optimization Results for [Me_2Zn]:

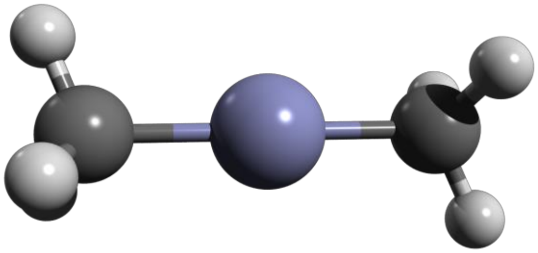

Figure S30. Optimized geometry of [Me_2Zn].

Zn	-1.31137494572970	0.25866524113407	0.00000881280284
C	0.63973821150303	0.25875163532231	-0.00023950767504
H	1.04670313248782	-0.22814763661916	0.91547520338332
H	1.04733598269605	-0.29056558584596	-0.87962906106343
H	1.04644760976925	1.29488026832544	-0.03587430172404
C	-3.26245947846385	0.25854767788404	0.00023462150814
H	-3.66996853151740	0.80628230159670	0.88065055634713
H	-3.66936023863871	0.74725928373924	-0.91454124109089
H	-3.66906174210649	-0.77767318553668	0.03391491751196

Optimization Results for [SnCp]$^+$:

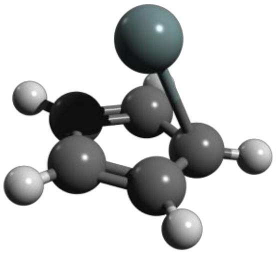

Figure S31. Optimized geometry of [CpSn]$^+$.

Sn	4.69395567884202	2.96127124303736	8.74863621789517
C	2.49020081647869	3.68672196754874	9.70062290002958
H	2.43599733801140	4.31157225373859	10.60476377220124
C	2.47237886626592	2.24887391125923	9.66536867579391
H	2.40233393736287	1.58203927534349	10.53789300452482
C	2.50050478835204	1.83747895880292	8.28715033788526
H	2.45533228277456	0.80090121894413	7.92096713324997
C	2.53648040033701	3.02122689142160	7.47127917226535
H	2.52270707072781	3.04842663399287	6.37087795560131
C	2.52952210236189	4.16414255307713	8.34419588388606
H	2.51006571848578	5.21816909283395	8.02892094666733

Optimization Results for [CpSnMe]:

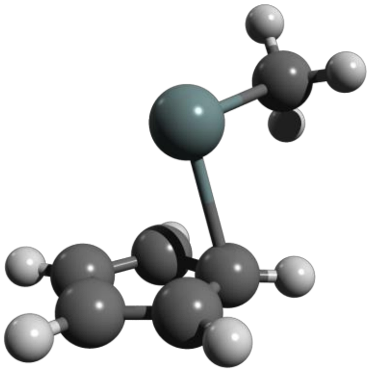

Figure S32. Optimized geometry of [CpSnMe].

C	3.25376268349257	3.65519538631061	9.30929325022313
H	3.73017716988496	4.25472562888211	10.10003987151081
C	3.18477537799588	2.20879863751749	9.26675750878546
H	3.60906419637864	1.52106116597088	10.01434959660364
C	2.26764813105605	1.85895150394887	8.21731710640220
H	2.00234126063681	0.83209028816053	7.92488548959183
C	1.77886859086772	3.04650585594602	7.62685374979371
H	1.09971728311220	3.10346864307355	6.76361890268837
C	2.38357231004874	4.14933136890121	8.27746732985669
H	2.21830199317885	5.21234250209312	8.04416824618566
Sn	5.00197892174804	2.92785924938624	7.72572020206217
C	6.66818552290116	2.92933033650240	9.25791184932767

H	7.51205959978302	2.29403093994019	8.90179806729936
H	7.06020844906471	3.96646406419900	9.38165679950916
H	6.34533850985065	2.56184442916777	10.25716203016016

Optimization Results for [(IMe)Ag(PhF)]$^{+}$:

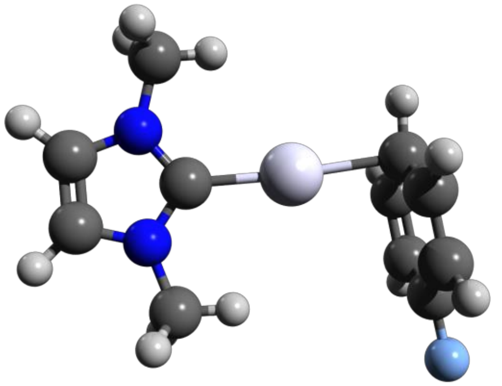

Figure S33. Optimized geometry of [(IMe)Ag(PhF)]$^{+}$.

Ag	9.81016047112574	12.63829711435420	4.70019412997542
F	9.20999439345450	12.07523831602001	9.47032179071914
N	12.02510032311857	14.81311848080584	4.41919186254966
N	11.38050897689331	14.12444909031303	2.46528014324365
C	11.16350726001223	13.94890938014458	3.80367988680707
C	12.76878441806672	15.51815841249686	3.48237115068998
H	13.51733496066447	16.26736865062334	3.76693557015754
C	12.36203694854695	15.08185230441580	2.24663925991561
H	12.68935916566946	15.37186838226986	1.24163174348909
C	8.93134944795677	11.76726279063604	8.20298463463271
C	9.64542808837593	10.72476963193010	7.58321993752446
H	10.40994699308399	10.17768701259437	8.15663693509947
C	9.34182663729387	10.38910449116581	6.25482115633841
H	9.85617082763848	9.53973947403568	5.77626153245474
C	8.32955446552331	11.09896901212615	5.54250825473946
H	7.96573607707514	10.71445330431688	4.57336025589219
C	7.63391850648394	12.16004065979312	6.19650191521900
H	6.81235608133227	12.68158275508142	5.67829366556726
C	7.93925697114921	12.49861607768734	7.52647191885794
H	7.40251025120579	13.30155271893674	8.05529160122535
C	12.14690215521725	15.00467747549366	5.86338500914358
H	13.20282668700650	14.86717150430758	6.17746783386526

H	11.80726295849209	16.02336771836391	6.14813608322366
H	11.51478551683015	14.25305400998881	6.37649304719736
C	10.70480602677358	13.39281559632012	1.39469781847324
H	11.41903052997260	12.71823654647827	0.87563519659120
H	9.88823270411750	12.78860522507999	1.83817062098301
H	10.27031215691974	14.10503386422048	0.66241704542455

Optimization Results for PhF:

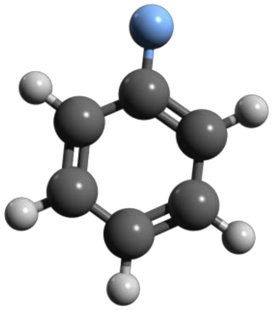

Figure S34. Optimized geometry of PhF.

C	-0.28980362666462	0.93913941811595	-0.00004157079355
C	1.11219871550981	0.96120437230347	0.00062788223536
C	1.83224780161706	2.16424331223309	0.00017063059307
C	1.12234515485782	3.37734691875069	-0.00098117644817
C	-0.28424751791048	3.38075752467126	-0.00165931114759
C	-0.98469157528034	2.16093718668622	-0.00119109226045
H	-0.81642603022712	-0.02850702608038	0.00034592447755
H	2.93392604870101	2.13556504089764	0.00072515991434
H	1.67896521572384	4.32961046250860	-0.00135294780068
H	-0.83550713095895	4.33538046461642	-0.00257379184333
H	-2.08812609858781	2.15558159772001	-0.00174172518919
F	1.78811904321978	-0.20725927242299	0.00167201826262

References

1. A. B. Pangborn, M. A. Giardello, R. H. Grubbs, R. K. Rosen, F. J. Timmers, *Organometallics*, 1996, **15**, 1518.

2. M. M. D. Roy, P. A. Lummis, M. J. Ferguson, R. McDonald, E. Rivard, *Chem. Eur. J.*, 2017, **23**, 11249.

3. (*a*) F. F. Puschmann, D. Stein, D. Heift, C. Hendriksen, Z. A. Gal, H. -F. Grützmacher, H. Grützmacher, *Angew. Chem. Int. Ed.*, 2011, **50**, 8420; (*b*) D. Heift, Z. Benkő, H. Grützmacher, *Dalton Trans.*, 2014, **43**, 831.

4. H. Hope, *Prog. Inorg. Chem.*, 1994, **41**, 1.

5. G. M. Sheldrick, *Acta. Crystallogr. Sect. A.*, 2015, **71**, 3.

6. G. M. Sheldrick, *Acta. Crystallogr. Sect. C.*, 2015, **71**, 3.

7. Gaussian 9, Revision D.01, M. J. Frisch, G. W. Trucks, H. B. Schlegel, G. E. Scuseria, M. A. Robb, J. R. Cheeseman, G. Scalmani, V. Barone, B. Mennucci, G. A. Petersson, H. Nakatsuji, M. Caricato, X. Li, H. P. Hratchian, A. F. Izmaylov, J. Bloino, G. Zheng, J. L. Sonnenberg, M. Hada, M. Ehara, K. Toyota, R. Fukuda, J. Hasegawa, M. Ishida, T. Nakajima, Y. Honda, O. Kitao, H. Nakai, T. Vreven, J. A. Montgomery, J. E. Peralta, F. Ogliaro, M. Bearpark, J. J. Heyd, E. Brothers, K. N. Kudin, V. N. Staroverov, R. Kobayashi, J. Normand, K. Raghavachari, A. Rendell, J. C. Burant, S. S. Iyengar, J. Tomasi, M. Cossi, N. Rega, J. M. Millam, M. Klene, J. E. Knox, J. B. Cross, V. Bakken, C. Adamo, J. Jaramillo, R. Gomperts, R. E. Stratmann, O. Yazyev, A. J. Austin, R. Cammi, C. Pomelli, J. W. Ochterski, R. L. Martin, K. Morokuma, V. G. Zakrzewski, G. A. Voth, P. Salvodor, J. J. Dannenberg, S. Dapprich, A. D. Daniels, Ö. Farkas, J. B. Foresman, J. V. Ortiz, J. Cioslowski, D. J. Fox, Gaussian, Inc., Wallingford CT, **2009**.

8. (*a*) C. Lee, W. Yang, R. G. Parr, *Phys. Rev. B*, 1988, **37**, 785; (*b*) A. D. Becke, *Phys. Rev. A*, 1988, **38**, 3098; (*c*) P. J. Stephens, F. J. Devlin, C. F. Chabalowski, M. J. Frisch, *J. Phys. Chem.*, 1994, **98**, 11623.

9. (*a*) P. C. Hariharan, J. A. Pople, *Theor. Chim. Acta*, **1973**, *28*, 213; (*b*) M. M. Francl, W. J. Pietro, W. J. Hehre, J. S. Binkley, M. S. Gordon, D. J. DeFrees, J. A. Pople, *J. Chem. Phys.*, 1982, **77**, 3654.

10. (*a*) P. J. Hay, W. R. Wadt, *J. Chem. Phys.*, 1985, **82**, 270; (*b*) W. R. Wadt, P. J. Hay, *J. Chem. Phys.*, 1985, **82**, 284; (*c*) P. J. Hay, W. R. Wadt, *J. Chem. Phys.*, 1985, **82**, 299.

11. F. Neese, *Wiley Interdiscip. Rev.: Comput. Mol. Sci.*, 2012, **2**, 73.

12. (*a*) A. D. Becke, *Phys. Rev. A.*, 1988, **38**, 3098; (*b*) J. P. Perdew, *Phys. Rev. B.*, 1986, **33**, 8822.

13. (*a*) F. Weigand, R. Ahlrichs, *Phys. Chem. Chem. Phys.*, 2005, **7**, 3297; (*b*) F. Weigand, *Phys. Chem. Chem. Phys.*, 2006, **8**, 1057.